Original Article

The roles of risk model based on the 3-XRCC genes in lung adenocarcinoma progression

Qun-Xian Zhang[1#], Ye Yang[2#], Heng Yang[1,3#], Qiang Guo[1], Jia-Long Guo[1,3], Hua-Song Liu[1], Jun Zhang[1], Dan Li[4]

[1]Department of Cardiothoracic Surgery, Taihe Hospital, Hubei University of Medicine, Shiyan, China; [2]Department of Psychiatry, Traditional Chinese Medicine Hospital of Shiyan, Shiyan, China; [3]Postgraduate Training Basement of Jinzhou Medical University, Taihe Hospital, Hubei University of Medicine, Shiyan, China; [4]Department of Oncology, Huanggang Central Hospital, Huanggang, China

Contributions: (I) Conception and design: D Li, J Zhang, QX Zhang; (II) Administrative support: J Zhang, JL Guo, HS Liu; (III) Provision of study materials or patients: Q Guo; (IV) Collection and assembly of data: Y Yang, H Yang; (V) Data analysis and interpretation: QX Zhang, Y Yang, H Yang, Q Guo; (VI) Manuscript writing: All authors; (VII) Final approval of manuscript: All authors.

[#]These authors contributed equally to this work.

Correspondence to: Dan Li. Department of Oncology, Huanggang Central Hospital, Huanggang 435300, China. Email: 804180423qq.com; Jun Zhang. Department of Cardiothoracic Surgery, Taihe Hospital, Hubei University of Medicine, Shiyan 442012, China. Email: 13508684276@139.com.

Background: The abnormal expression of deoxyribonucleic acid (DNA) repair genes might be the cause of tumor development and resistance of malignant cells to chemotherapeutic drugs. A risk model based on the X-ray repair of cross-complementary (*XRCC*) genes was constructed to improve the diagnosis and treatment of lung adenocarcinoma (LUAD) patients.

Methods: The expression levels, diagnostic values, and prognostic values of *XRCC* genes were identified, and the roles and regulatory mechanisms of the risk model based on the *XRCC4/5/6* in LUAD progression was explored via The Cancer Genome Atlas (TCGA) and Oncomine databases.

Results: *XRCC1/2/3/4/5/6*, *XRCC7* (*PRKDC*), and *XRCC9* (*FANCG*) were overexpressed, and had diagnostic value for LUAD. The *XRCC* genes were involved in DNA repair, and participated in the regulation of non-homologous end-joining, homologous recombination, etc. The overall survival (OS), tumor (T) stage, and survival status of patients were significantly different between the Cluster1 and Cluster2 groups. *XRCC4/5/6* were independent risk factors affecting the prognosis of LUAD patients. The risk score was related to the prognosis, sex, clinical stage, T, lymph node (N), and metastasis (M) stage, as well as the survival status of LUAD patients. The clinical stage and risk score were independent risk factors for poor prognosis in LUAD patients. The risk model was involved in RNA degradation, cell cycle, basal transcription factors, DNA replication etc. The risk scores were significantly correlated with the expression levels of *TGFBR1*, *CD160*, *TNFSF4*, *TNFRSF14*, *IL6R*, *CXCL16*, *TNFRSF25*, *TAPBP*, *CCL16*, and *CCL14*.

Conclusions: The risk model based on the *XRCC4/5/6* genes could predict the progression of LUAD patients.

Keywords: *XRCC4*; *XRCC5*; *XRCC6*; lung adenocarcinoma (LUAD); prognosis

Submitted Jul 12, 2021. Accepted for publication Aug 26, 2021.
doi: 10.21037/tcr-21-1431
View this article at: https://dx.doi.org/10.21037/tcr-21-1431

Introduction

The deoxyribonucleic acid (DNA) repair system plays a vital role in protecting the human genome from carcinogens. The abnormal expression of DNA repair genes might be the cause of tumor development and resistance of malignant cells to chemotherapeutic drugs (1-6). For example, hydroxycamptothecin (*HCPT*) could increase the expression of the DNA repair gene, *XPF*, in bladder

cancer and promote apoptosis in T24 and 5637 cells. The increased expression of *XPF* could reduce the sensitivity of bladder cancer cells, while interfering with the expression of *XPF* could reduce the resistance of bladder cancer cells to chemotherapy (5). Likewise, interfering with the expression of *BRCA1* interacting protein C-terminal helicase 1 (*BRIP1)*, which regulates DNA repair and cell proliferation could induce cell cycle arrest and reduce the proliferation of breast cancer (BC) cells, and promote the invasion of BC cells (6). These examples highlight the important role of the DNA repair system in cancer progression.

The X-ray repair of cross-complementary (*XRCC)* genes are common components of the DNA repair system and are related to cancer progression. For example, *XRCC1* is essential for DNA base excision repair, single strand break repair, and nucleotide excision repair. In ovarian cancer, *XRCC1* is positive in 48% of tumor patients, which is related to advanced stage, platinum resistance, disease progression, and so on. The expression level of *XRCC1* is an independent risk factor for cancer specificity and progression-free survival. Compared with *XRCC1*-positive cells, *XRCC1*-negative cells are sensitive to cisplatin, which is related to DNA double-strand breaks and cell cycle arrest of G2/M (7). *XRCC2* overexpression has been found in rectal cancer tissues without preoperative radiotherapy (PRT). Compared with *XRCC2*-positive patients treated with PRT, XRCC2-negative patients with locally advanced rectal cancer (LARC) have improved overall survival (OS). The level of *XRCC2* expression is related to the increase of radiation resistance of LARC, while cancer cells without *XRCC2* expression are more sensitive to radiation *in vitro*, which is related to the arrest and apoptosis of cells in the G2/M phase. When the expression of *XRCC2* is interfered with, the repair ability of DNA double strand breaks caused is impaired via radiation (8).

The Cancer Genome Atlas (TCGA) database aims to apply high-throughput genome analysis technology to improve people's ability to prevent, diagnose, and treat cancer. It has multiple cancer types and groups of data, including gene expression data, microRNA (miRNA) expression data, copy number variation, DNA methylation, and so on (9,10). However, the role of *XRCC* genes in the progression of lung adenocarcinoma (LUAD) has not been fully elucidated. In recent years, risk models have also been commonly used to assess the prognosis of cancer patients (11,12). In this study, the expression levels, diagnostic value, and prognostic value of *XRCC* genes in LUAD were evaluated using the Oncomine and TCGA databases, and a risk model was constructed to evaluate the clinical predictive value for the progression of LUAD patients. The following article was presented in accordance with the TRIPOD reporting checklist (available at https://dx.doi.org/10.21037/tcr-21-1431).

Methods

The study was conducted in accordance with the Declaration of Helsinki (as revised in 2013).

Oncomine database

The Oncomine 3.0 (https://www.oncomine) database is used for the study of tumor-related genes, with a wide range of data sources and high reliability (13). The expression of *XRCC* genes in pan-cancer tissues was analyzed in the Oncomine database. The *XRCC* genes included the following: *XRCC1*, *XRCC2*, *XRCC3*, *XRCC4*, *XRCC5*, *XRCC6*, *FANCG*, and *PRKDC*. The screening criteria were as follows: (I) genes: *XRCC1/2/3/4/5/6*, *FANCG*, and *PRKDC*; (II) analysis type: cancer versus normal analysis; (III) data type: messenger RNA (mRNA); (IV) $P<0.05$; and (V) fold change: ALL.

Visualization analysis of TCGA data

The gene expression data of HTSeq-FPKM tissue, including 59 cases of lung tissues and 535 cases of LUAD tissues, and the clinical data of 522 cancer patients were downloaded from the official TCGA (https://portal.gdc.cancer.gov/projects/TCGA-LUAD (HTSeq-FPKM) website. Among them, 57 lung tissues and 57 LUAD tissues were derived from the same LUAD patients. The expressions of *XRCC1/2/3/4/5/6*, *FANCG*, and *PRKDC* were identified in lung and LUAD tissues, and the correlation between *XRCC* genes was analyzed. Principal component analysis (PCA), gene set enrichment analysis (GSEA), and clinical correlation analysis were performed in the 535 cases of LUAD issues.

Consensus clustering and survival analysis

According to the expression levels of *XRCC* genes, the 535 cases of LUAD tissues in TCGA database were divided into two groups using the "Consensus-ClusterPlus" in R, and PCA was performed (14,15). Kaplan-Meier survival analysis and correlation analysis were performed to evaluate the OS and

clinicopathological characteristics (age, sex, clinical stage, T stage, N stage, M stage, and survival status) in both groups.

Construction of the risk model in LUAD

Univariate Cox regression analysis was used to filter the prognostic factors in patients with LUAD. The independent risk factors for poor prognosis of LUAD patients were screened by multivariate Cox regression analysis and the Akaike information criterion (AIC) (16). LUAD patients were divided into high- and low-risk groups according to the gene expression levels. Kaplan-Meier survival analysis evaluated the risk of death in two groups of LUAD patients. The relationship between risk and clinicopathological features (including age, sex, clinical stage, T stage, N stage, M stage) was assessed in patients with LUAD via correlation analysis.

The value of risk model in the prognosis of LUAD

Univariate and multivariate Cox regression analyses were used to assess the effects of the risk model, age, sex, clinical stage, T stage, N stage, and M stage on the prognosis of LUAD patients, and to evaluate the role of the risk model in the prognosis of LUAD patients (17).

Biological processes and signaling mechanisms

The *XRCC* genes were entered into the String (https://string-db.org) database to conduct Gene Ontology (GO), Kyoto Encyclopedia of Genes and Genomes (KEGG), and protein-protein interaction (PPI) analyses. GSEA was used to explore the biological functions and regulatory mechanisms that the influencing factors might be involved in (18-20). The LUAD tissue gene expression data from TCGA database were divided into high- and low-risk groups according to the median value of the risk model score to explore the effects of two groups on each gene. GO [biological process (BP)] and KEGG analyses were carried out using the GSEA software. The screening criteria was as follows: nominal (NOM) P<0.05.

Correlation analysis of LUAD immune cell markers

The relationship between risk model factors and LUAD immune infiltrating cell markers were analyzed in 535 cases of LUAD via correlation analysis. One-to-one correspondence between the risk score and LUAD samples was conducted. The expression level of LUAD immune infiltrating cell markers were explored in the high- and low-risk groups.

Statistical analysis

Cox regression and Kaplan-Meier survival analysis were used to analyze the risk factors associated with OS in patients with LUAD. The univariate and multivariate Cox regression analyses and AIC were used to screen the prognostic factors in patients with LUAD. Correlation analysis was used to analyze the relationship between the risk factors and LUAD immune cell infiltration markers. GraphPrism 5.0 and R (Version 3.6.1) ggplot package were plotted. P<0.05 was regarded as statistically significant.

Results

The expression level of XRCC genes was significantly increased in LUAD tissues

In the Oncomine database, *XRCC1*, *XRCC2*, *XRCC3*, *XRCC4*, *XRCC5*, *XRCC6*, *FANCG*, and *PRKDC* were abnormally expressed in pan-cancer tissues, and the expression levels of *XRCC* genes were mainly increased in pan-cancer tissues (Figure S1). Based on our screening criteria, most of the datasets showed that *XRCC* genes were predominantly higher in lung cancer tissues. Specifically, the datasets related to the expression of *XRCC1*, *XRCC6*, *XRCC2*, *XRCC3*, *FANCG*, *XRCC4*, *XRCC5*, and *PRKDC* were 4 *vs.* 1, 9 *vs.* 5, 5 *vs.* 4, 13 *vs.* 0, 14 *vs.* 3, 8 *vs.* 0, 13 *vs.* 4, and 18 *vs.* 2, respectively.

In addition, the expression levels of *XRCC1*, *XRCC6*, *XRCC3*, *XRCC2*, *FANCG*, *XRCC4*, *XRCC5*, and *PRKDC* increased in LUAD tissues in the TCGA database, and the difference was statistically significant (*Figure 1*). In addition, we sorted the data obtained from the TCGA database and matched the tissues one-to-one to show that the expression levels of *XRCC1*, *XRCC6*, *XRCC3*, *XRCC2*, *FANCG*, *XRCC4*, *XRCC5*, and *PRKDC* increased in LUAD tissues (*Figure 2*).

Diagnostic value of XRCC genes in LUAD

The diagnostic value of *XRCC* genes in LUAD was evaluated via receiver operator characteristic (ROC) analysis. The results showed that the area under the curve (AUC) of *XRCC1*, *XRCC6*, *XRCC2*, *XRCC3*, *FANCG*, *XRCC4*, *XRCC5*, and *PRKDC* were all between 0.5 and 1, which was statistically significant (*Figure 3*). Specifically,

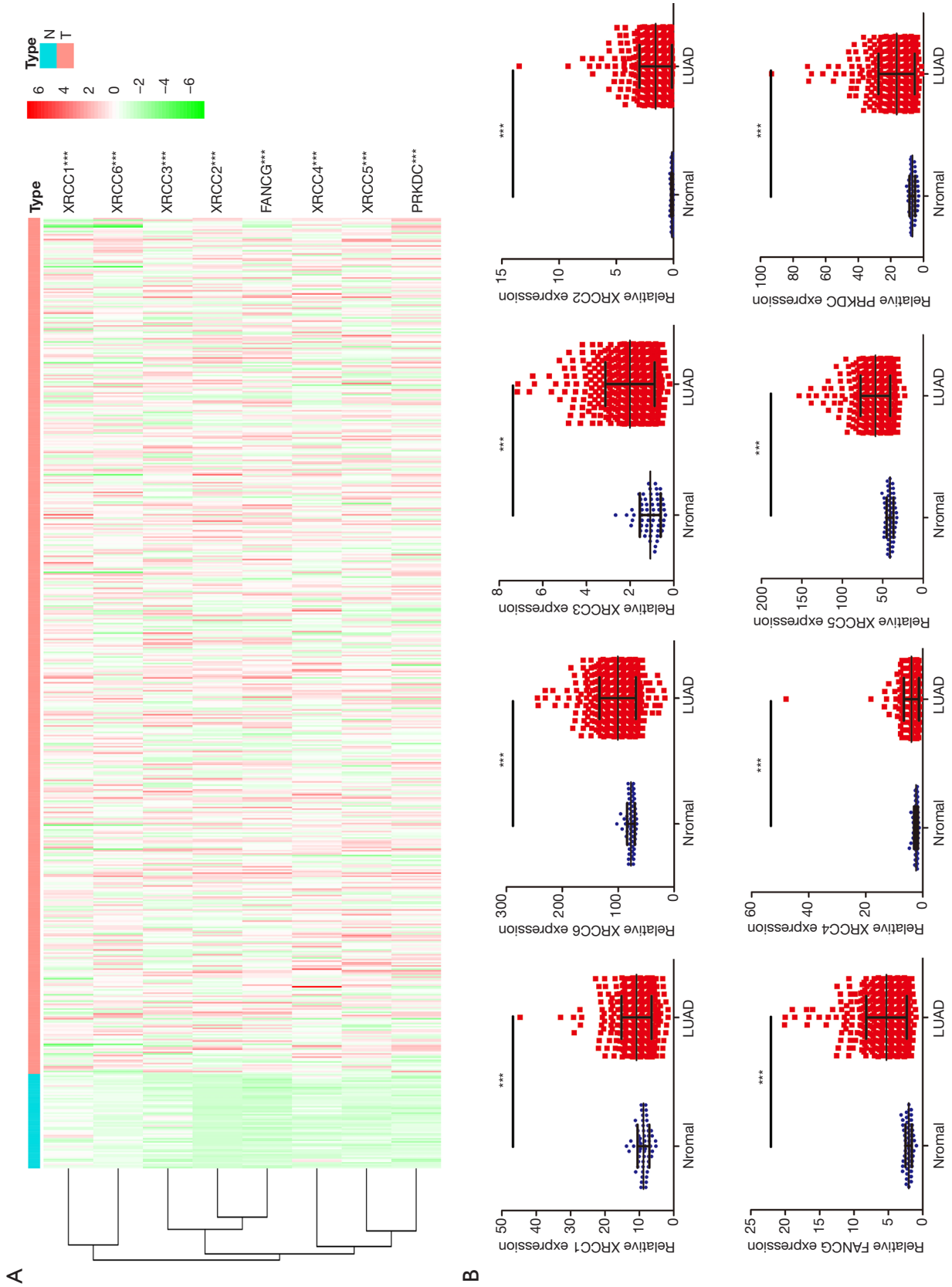

Figure 1 High expression of *XRCC* genes in TCGA LUAD tissues. (A) Heat map showing the expression of *XRCC* genes in LUAD tissues; (B) scatter plot showing the expression of *XRCC* genes in LUAD tissues. XRCC, X-ray repair of cross-complementary; TCGA, The Cancer Genome Atlas; LUAD, lung adenocarcinoma. ***, P<0.001.

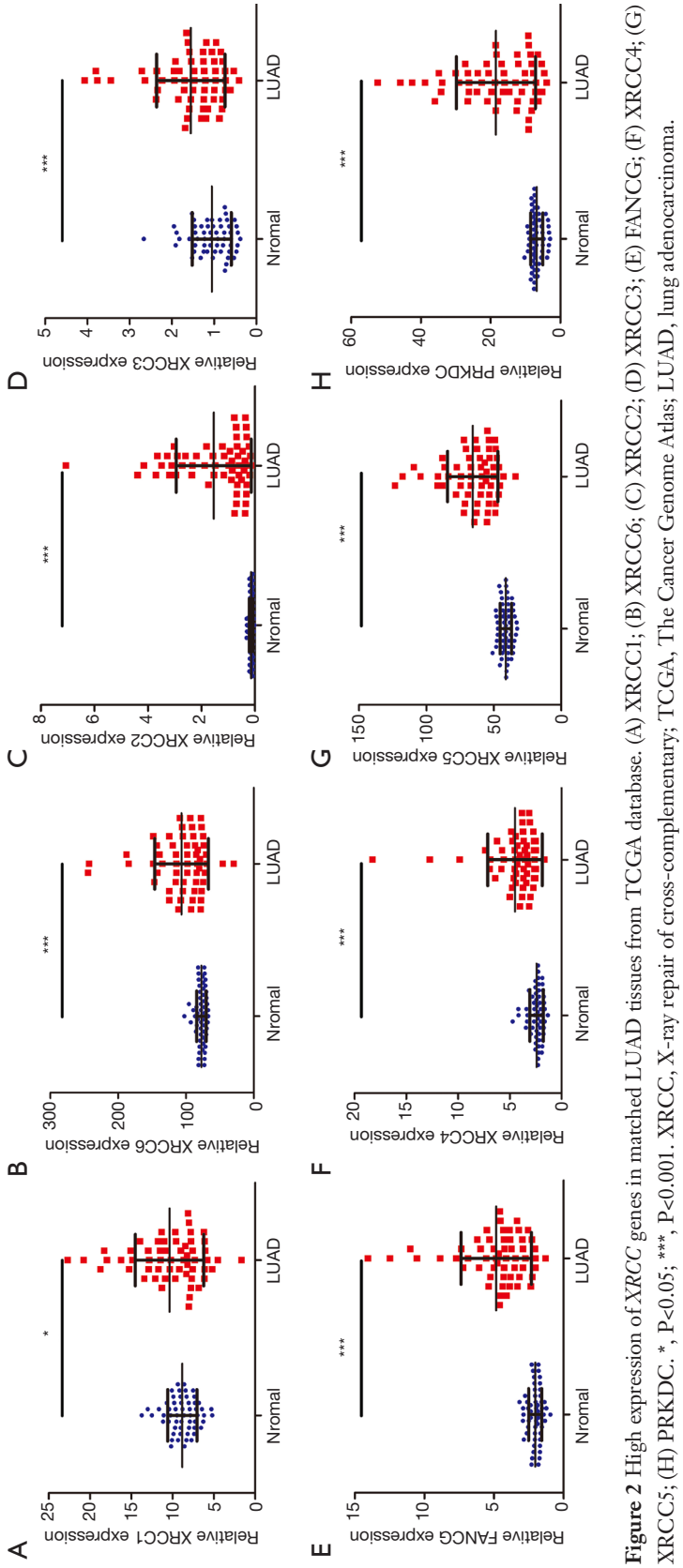

Figure 2 High expression of *XRCC* genes in matched LUAD tissues from TCGA database. (A) XRCC1; (B) XRCC6; (C) XRCC2; (D) XRCC3; (E) FANCG; (F) XRCC4; (G) XRCC5; (H) PRKDC. *, P<0.05; ***, P<0.001. XRCC, X-ray repair of cross-complementary; TCGA, The Cancer Genome Atlas; LUAD, lung adenocarcinoma.

the AUCs of *XRCC1*, *XRCC6*, *XRCC2*, *XRCC3*, *FANCG*, *XRCC4*, *XRCC5*, and *PRKDC* were 0.6628 (*Figure 3A*), 0.7785 (*Figure 3B*), 0.9841 (*Figure 3C*), 0.7913 (*Figure 3D*), 0.9943 (*Figure 3E*), 0.8425 (*Figure 3F*), 0.8743 (*Figure 3G*), and 0.8732 (*Figure 3H*), respectively.

The biological functions of XRCC genes

In LUAD tissues, we observed significant correlations between the expression levels of the following genes: (I) *XRCC1* and *XRCC3*, and *FANCG* and *XRCC4*; (II) *XRCC3* and *FANCG* and *XRCC2*; (III) *FANCG* and *XRCC5*, and *XRCC2* and *PRKDC*; (IV) *XRCC5* and *XRCC6*, and *XRCC2* and *PRKDC*; and (V) *XRCC2* and *PRKDC* (Figure S2A). Using the String database, we found that *XRCC* genes were involved in biological processes such as DNA repair, DNA recombination, response to radiation, response to X-ray, mitotic recombination, and so on, and were also involved in the regulation of non-homologous end-joining and homologous recombination signaling mechanisms (*Tables 1-3* and Table S1). In the PPI network, there was a strong functional relationship among the *XRCC* genes (Figure S2B).

Consensus clustering of XRCC genes identified two clusters of LUAD with different clinical outcomes

With the evolution of clustering from k=2 to 9, k=2 might be the best choice with the least interference in our clustering (*Figure 4A-4C*). Therefore, we used k=2 for consensus clustering analysis, and defined it as Cluster1 and Cluster2 groups. PCA was performed in the 535 cases of LUAD from the TCGA database, and the results showed that there was a significant difference between the Cluster1 and Cluster2 groups (*Figure 4D*). Survival analysis showed that the OS of LUAD patients in Cluster1 was better than that of LUAD patients in Cluster2 (*Figure 4E*). Correlation analysis showed that there was a significant correlation between T stage and survival status of patients in the Cluster1 and Cluster2 groups (*Figure 4F*).

The prognostic value of XRCC genes in patients with LUAD

The value of *XRCC* genes in the prognosis of LUAD was explored via univariate Cox regression analysis. We found that *XRCC4*, *XRCC5*, *XRCC6*, and *PRKDC* might be the risk factors affecting the prognosis of LUAD patients (*Figure 5A*). On this basis, the risk model was constructed under the conditions of multivariate Cox regression analysis and AIC optimization. The results showed that *XRCC4*, *XRCC5*, and *XRCC6* were independent risk factors affecting the prognosis of patients with LUAD. Kaplan-Meier survival analysis showed that the prognosis of LUAD patients in the high-risk group was worse (*Figure 5B*). Correlation analysis showed that high- and low-risk were significantly correlated with the gender, clinical stage, T stage, N stage, M stage, and survival status of LUAD patients (*Figure 5C*). The univariate and multivariate Cox regression analyses showed that the clinical stage and risk score were independent risk factors for poor prognosis in patients with LUAD (*Figure 6*).

The biological functions and signaling pathways involved in the risk model

According to the median risk score, we divided the gene expression data of the 535 cases of LUAD from the TCGA into high- and low-risk groups to explore the influence of genes in two groups. The GSEA results showed that increased risk might involve biological processes such as regulation of DNA replication, mitotic metaphase plate congression, cell cycle DNA replication (Figure S3), as well as signaling systems such as RNA degradation, cell cycle, oocyte meiosis, basal transcription factors, and DNA replication (Figure S4 and *Table 4*).

The risk model based on XRCC4, XRCC5, and XRCC6 was related to the LUAD immunity

The correlation analysis showed that *XRCC4*, *XRCC5*, *XRCC6*, and their risk model were significantly correlated with the levels of immune factors (*Figures 7,8*). Specifically, the expression level of *XRCC4* was positively correlated with the expression levels of *TNFSF4*, *CD80*, *PDCD1LG2*, *CXCL8*, etc. (*Figure 7A* and Table S2), and negatively correlated with the expression levels of *CXCL17*, *IL6R*, *TAPBP*, *CXCL16*, etc. (*Figure 7B* and Table S2). The expression level of *XRCC5* was positively correlated with the expression levels of *PVR*, *TGFBR1*, *CXCL8*, *XCL1*, etc. (*Figure 7C* and Table S2), and negatively correlated with the expression levels of *TNFRSF14*, *HLA-DMA*, *TMEM173*, *HLA-DPB1*, etc. (*Figure 7D* and Table S2). The expression level of *XRCC6* was positively correlated with the expression levels of *CD276*, *TNFSF13*, *CXCL16*, *TNFSF9*, etc. (*Figure 7E* and Table S2), and negatively correlated with the expression levels of *CD160*, *KLRK1*, *BTLA*, *CCL16*, etc.

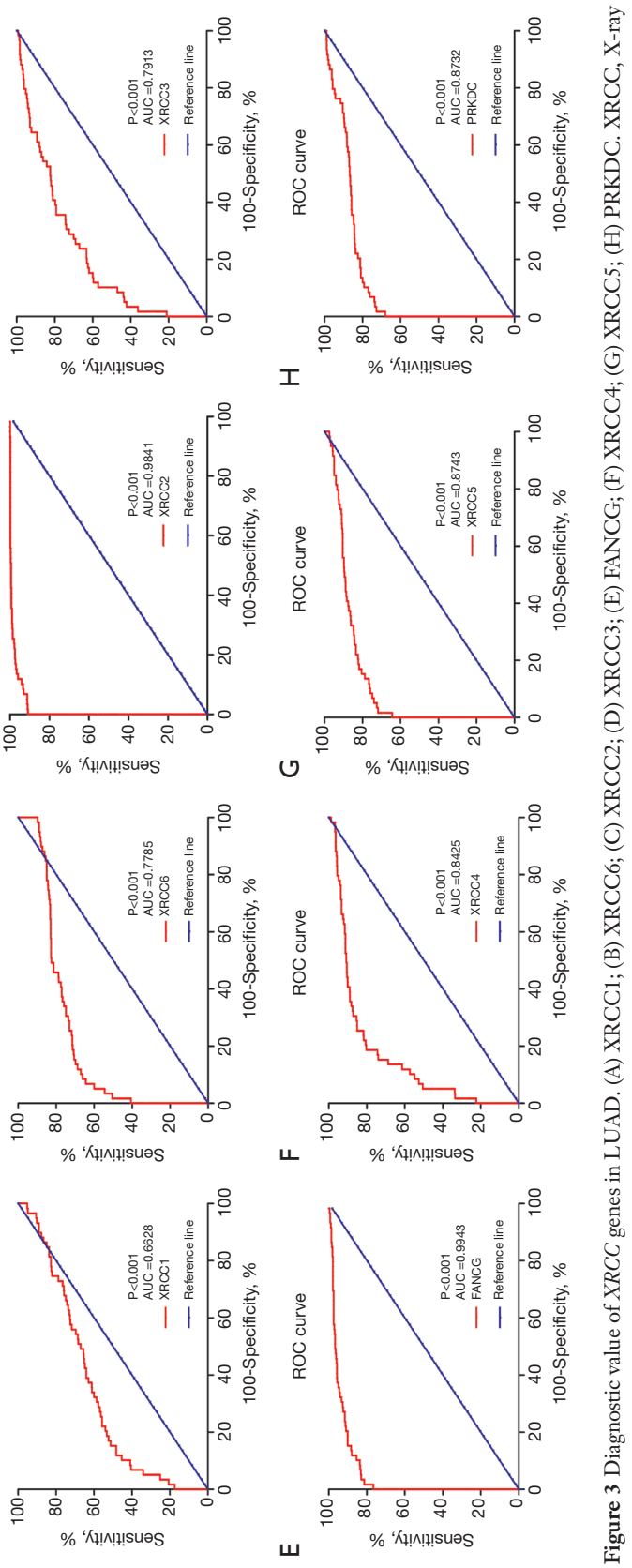

Figure 3 Diagnostic value of *XRCC* genes in LUAD. (A) XRCC1; (B) XRCC6; (C) XRCC2; (D) XRCC3; (E) FANCG; (F) XRCC4; (G) XRCC5; (H) PRKDC. XRCC, X-ray repair of cross-complementary; LUAD, lung adenocarcinoma; ROC, receiver operator characteristic; AUC, the area under the curve.

Table 1 The *XRCC* genes were involved in biological processes

GO: BP	Description	P
GO:0006302	Double-strand break repair	2.94E-11
GO:0006281	DNA repair	3.49E-11
GO:0006310	DNA recombination	3.49E-11
GO:0010212	Response to ionizing radiation	7.62E-10
GO:0009314	Response to radiation	1.68E-09
GO:0006303	Double-strand break repair via nonhomologous end joining	2.33E-09
GO:0009628	Response to abiotic stimulus	4.44E-09
GO:0000723	Telomere maintenance	1.31E-08
GO:0010165	Response to X-ray	3.56E-08
GO:0010332	Response to gamma radiation	2.12E-07
GO:0075713	Establishment of integrated proviral latency	2.84E-07
GO:0006266	DNA ligation	1.33E-06
GO:0006312	Mitotic recombination	2.32E-06
GO:0071475	Cellular hyperosmotic salinity response	3.91E-05
GO:0032481	Positive regulation of type I interferon production	5.69E-05
GO:0000707	Meiotic DNA recombinase assembly	0.00012
GO:0000724	Double-strand break repair via homologous recombination	0.00012
GO:0051351	Positive regulation of ligase activity	0.00012
GO:0042148	Strand invasion	0.00013
GO:0000722	Telomere maintenance via recombination	0.00019
GO:0051103	DNA ligation involved in DNA repair	0.00019
GO:0071481	Cellular response to X-ray	0.00019
GO:0048660	regulation of smooth muscle cell proliferation	0.00021
GO:0006996	Organelle organization	0.00024
GO:0002218	Activation of innate immune response	0.00057
GO:0071480	Cellular response to gamma radiation	0.00069
GO:0007420	Brain development	0.00087
GO:0032205	Negative regulation of telomere maintenance	0.0012
GO:0007131	Reciprocal meiotic recombination	0.0017
GO:0036297	Interstrand cross-link repair	0.0017
GO:0032508	DNA duplex unwinding	0.002
GO:0033044	Regulation of chromosome organization	0.002
GO:0001756	Somitogenesis	0.0027
GO:0043902	Positive regulation of multi-organism process	0.0035
GO:0002244	Hematopoietic progenitor cell differentiation	0.0037
GO:0007399	Nervous system development	0.0054
GO:0080134	Regulation of response to stress	0.0074

Table 1 (*continued*)

Table 1 (*continued*)

GO: BP	Description	P
GO:0022414	Reproductive process	0.0083
GO:0043085	Positive regulation of catalytic activity	0.0086
GO:0051704	Multi-organism process	0.0086

XRCC, X-ray repair of cross-complementary; GO, Gene Ontology; BP, biological process.

Table 2 The *XRCC* genes were involved in molecular function

GO: MF	Description	P
GO:0140097	Catalytic activity, acting on DNA	2.35E-07
GO:0003684	Damaged DNA binding	3.37E-07
GO:0008094	DNA-dependent ATPase activity	3.37E-07
GO:0003677	DNA binding	6.46E-05
GO:0000150	Recombinase activity	0.0001
GO:0003690	Double-stranded DNA binding	0.0001
GO:0008022	Protein C-terminus binding	0.00044
GO:0005524	ATP binding	0.00074
GO:0042162	Telomeric DNA binding	0.00074
GO:0003678	DNA helicase activity	0.00078
GO:0008144	Drug binding	0.00088
GO:0003697	Single-stranded DNA binding	0.0019
GO:0016787	Hydrolase activity	0.003

XRCC, X-ray repair of cross-complementary; GO, Gene Ontology; MF, molecular function.

Table 3 The *XRCC* genes were involved in cellular component

GO: CC	Description	P
GO:1990391	DNA repair complex	6.40E-11
GO:0070419	Nonhomologous end joining complex	2.57E-10
GO:0000784	Nuclear chromosome, telomeric region	8.13E-08
GO:0005654	Nucleoplasm	1.10E-05
GO:0043564	Ku70:Ku80 complex	1.10E-05
GO:0005958	DNA-dependent protein kinase-DNA ligase 4 complex	1.97E-05
GO:0033063	Rad51B-Rad51C-Rad51D-XRCC2 complex	2.58E-05
GO:0005730	Nucleolus	6.28E-05
GO:0005694	Chromosome	6.31E-05
GO:0032991	Protein-containing complex	6.31E-05
GO:0000783	Nuclear telomere cap complex	6.43E-05
GO:0032993	Protein-DNA complex	0.00015
GO:0043232	Intracellular non-membrane-bounded organelle	0.00028
GO:0005657	Replication fork	0.00056

XRCC, X-ray repair of cross-complementary; GO, Gene Ontology; CC, cellular component.

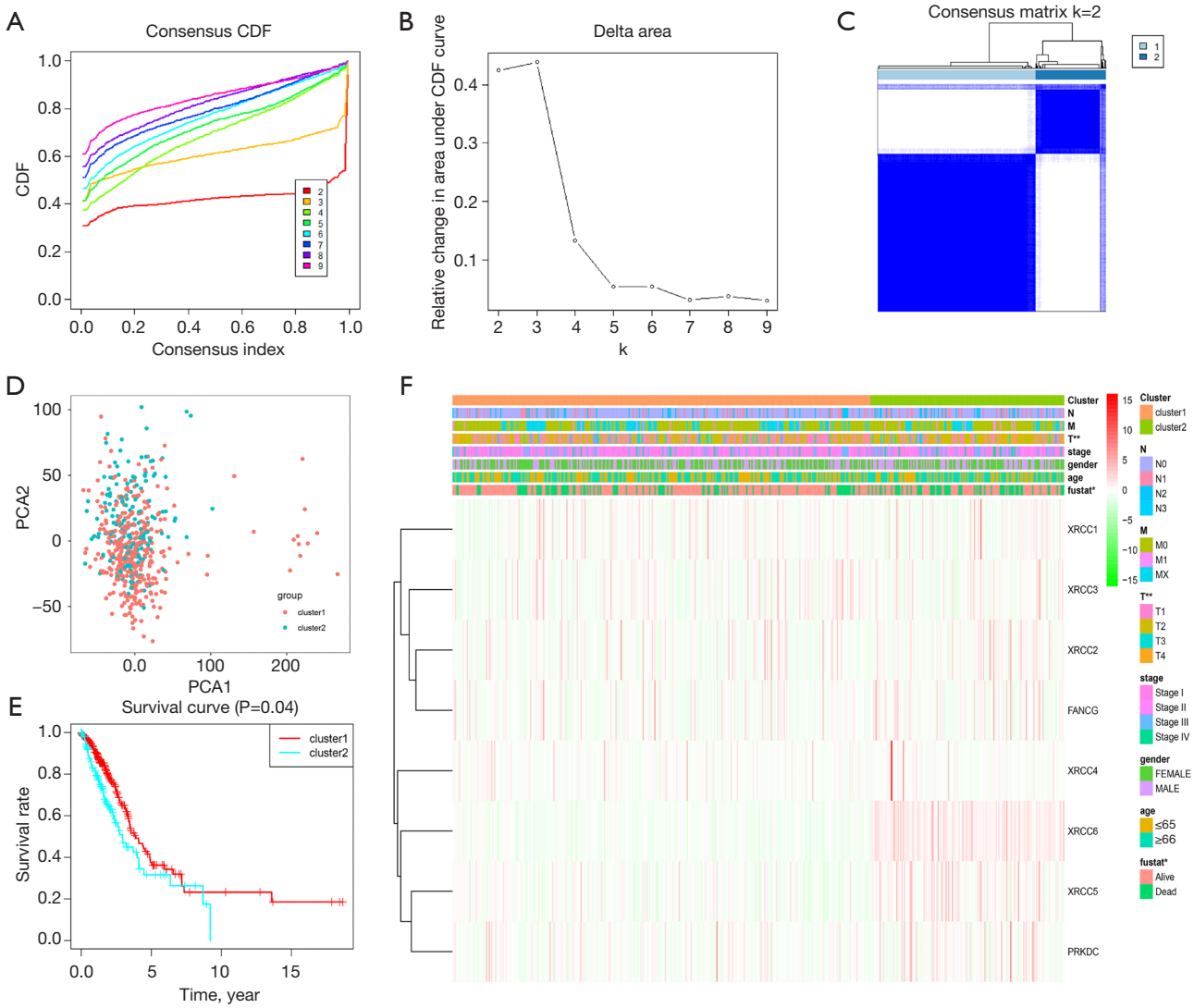

Figure 4 The overall survival of LUAD patients in the Cluster1 and Cluster2 subgroups. *, P<0.05; **, P<0.01. LUAD, lung adenocarcinoma.

(*Figure 7F* and Table S2).

The immune factors associated with the intersection of *XRCC4*, *XRCC5*, and *XRCC6* in both high- and low-risk groups were validated (*Figure 8A*). Specifically, the expression levels of *TGFBR1*, *CD160*, *TNFSF4*, *TNFRSF14*, *IL6R*, *CXCL16*, *TNFRSF25*, *TAPBP*, *CCL16*, and *CCL14* were significantly associated with high- and low-risk scores (*Figure 8B-8K*).

Discussion

Persistent failure to repair DNA damage might lead to cell cycle arrest, apoptosis, and genomic instability, which leads to the development of many diseases (21). The *XRCC* genes are important components of the DNA damage repair mechanism and play important biological roles in cancer progression (21-24). At present, numerous studies have confirmed that polymorphisms of DNA damage repair genes such as XRCC1, XRCC3, and XRCC4 were associated with the survival of patients with lung cancer (25-27). However, the role of *XRCC* genes in the progression of LUAD has not been fully elucidated. In this study, we observed that the expression levels of XRCC1, XRCC6, XRCC3, XRCC2, FANCG, XRCC3, XRCC4,

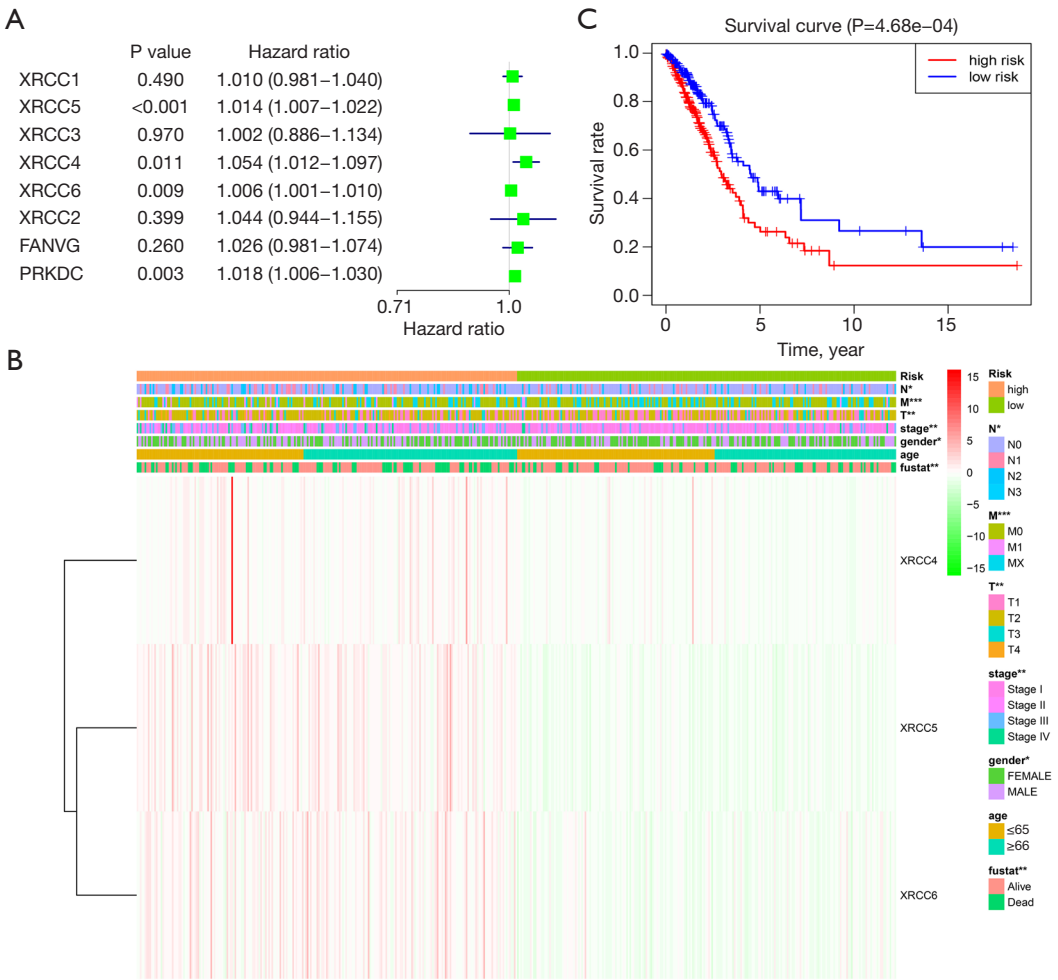

Figure 5 Prognostic value of *XRCC* genes in patients with LUAD. (A) Univariate Cox regression analysis; (B,C) risk score was correlated to the clinicopathological features and OS of LUAD patients based on XRCC4, XRCC5, and XRCC6. *, P<0.05; **, P<0.01; ***, P<0.001. XRCC, X-ray repair of cross-complementary; LUAD, lung adenocarcinoma; OS, overall survival.

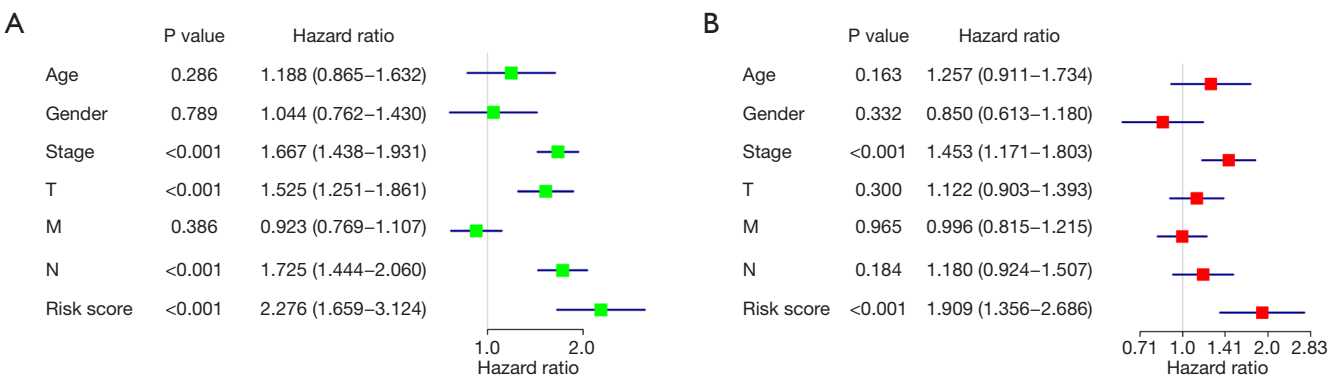

Figure 6 Univariate and multivariate Cox regression analysis revealed that the clinical stage and risk score were independent risk factors for poor prognosis in patients with LUAD. (A) Univariate Cox regression analysis; (B) multivariate Cox regression analysis. LUAD, lung adenocarcinoma.

Table 4 The high-risk group was involved in signaling pathways via the GSEA

Name	Size	NES	NOM P value
RNA_degradation	57	2.1544359	0
Cell_cycle	124	2.139343	0
Nucleotide_excision_repair	44	2.1303906	0.001964637
OOCYTE_MEIOSIS	112	2.0731578	0.001996008
Mismatch_repair	23	2.0708838	0
Basal_transcription_factors	35	2.0075533	0
DNA_replication	36	1.98874	0
Proteasome	44	1.9682256	0.001972387
Ubiquitin_mediated_proteolysis	133	1.9554849	0
Protein_export	23	1.9503225	0
pathogenic_escherichia_coli_infection	55	1.9071776	0.005825243
Citrate_cycle_tca_cycle	30	1.8967364	0.004056795
Spliceosome	126	1.890303	0.004032258
Pyrimidine_metabolism	98	1.8573432	0.00204499
Purine_metabolism	157	1.8310792	0.002159827
Cysteine_and_methionine_metabolism	34	1.7912648	0.003861004
P53_signaling_pathway	68	1.733961	0.007843138
One_carbon_pool_by_folate	17	1.7224773	0.016129032
RNA_polymerase	29	1.7176231	0.018367346
Homologous_recombination	28	1.6963832	0.034274194
Biosynthesis_of_unsaturated_fatty_acids	22	1.6282122	0.018072288
Riboflavin_metabolism	15	1.620054	0.036538463
Aminoacyl_trna_biosynthesis	22	1.5583364	0.049701788
Progesterone_mediated_oocyte_maturation	85	1.4684261	0.07370518
Amyotrophic_lateral_sclerosis_als	52	1.4148762	0.047244094
Glyoxylate_and_dicarboxylate_metabolism	16	1.3979565	0.115686275
Glycolysis_gluconeogenesis	62	1.388122	0.082
Huntingtons_disease	177	1.3863257	0.14256199
Terpenoid_backbone_biosynthesis	15	1.378746	0.14141414
Pentose_phosphate_pathway	27	1.3762755	0.1097561
Thyroid_cancer	29	1.3680532	0.091617934
Pancreatic_cancer	70	1.3660588	0.11133201
Adherens_junction	73	1.3573757	0.11576846
Base_excision_repair	33	1.34626	0.17886178
Alzheimers_disease	163	1.3419145	0.15352698
Tgf_beta_signaling_pathway	85	1.3412957	0.11025145

Table 4 (*continued*)

Table 4 (*continued*)

Name	Size	NES	NOM P value
N_glycan_biosynthesis	46	1.3321104	0.1482966
Colorectal_cancer	62	1.3087744	0.14705883
Propanoate_metabolism	31	1.2553445	0.2300195
Glycosylphosphatidylinositol_gpi_anchor_biosynthesis	25	1.2523328	0.22113504
WNT_signaling_pathway	150	1.2449616	0.14
Chronic_myeloid_leukemia	73	1.227265	0.21370968
Small_cell_lung_cancer	84	1.197284	0.23203285
Epithelial_cell_signaling_in_helicobacter_pylori_infection	68	1.1845227	0.20315582
Prostate_cancer	89	1.1837994	0.23883495
Pathways_in_cancer	325	1.1785803	0.20081967
Renal_cell_carcinoma	70	1.164982	0.24055666
Long_term_potentiation	70	1.1516585	0.23943663
Cytosolic_dna_sensing_pathway	54	1.1250238	0.31769723
Ribosome	87	1.1220671	0.43037975
Nicotinate_and_nicotinamide_metabolism	24	1.1175917	0.28849903
Regulation_of_actin_cytoskeleton	212	1.1145742	0.27991885
Parkinsons_disease	125	1.089907	0.39793813
Vasopressin_regulated_water_reabsorption	44	1.0887667	0.33466136
Glutathione_metabolism	47	1.0859108	0.36452243
Lysine_degradation	44	1.0843796	0.34068137
Snare_interactions_in_vesicular_transport	38	1.0831342	0.33714285
Valine_leucine_and_isoleucine_degradation	43	1.0764002	0.38446215
Pyruvate_metabolism	40	1.0609999	0.3767821
Pentose_and_glucuronate_interconversions	28	1.0568165	0.41497976
Selenoamino_acid_metabolism	25	1.0436656	0.38202247
Rig_i_like_receptor_signaling_pathway	70	1.0409458	0.3732535
Regulation_of_autophagy	35	1.0247588	0.4329502
Amino_sugar_and_nucleotide_sugar_metabolism	43	1.022107	0.4027778
Peroxisome	78	1.0060785	0.4322709
Melanoma	71	1.003775	0.44466403
Nod_like_receptor_signaling_pathway	62	1.0017914	0.46601942
Alanine_aspartate_and_glutamate_metabolism	30	0.98454267	0.47233203
Endocytosis	181	0.9828535	0.45691383
Fructose_and_mannose_metabolism	33	0.9741695	0.46626985
Glioma	65	0.9564347	0.49203187

GSEA, gene set enrichment analysis; NES, normalized enrichment score; NOM, nominal.

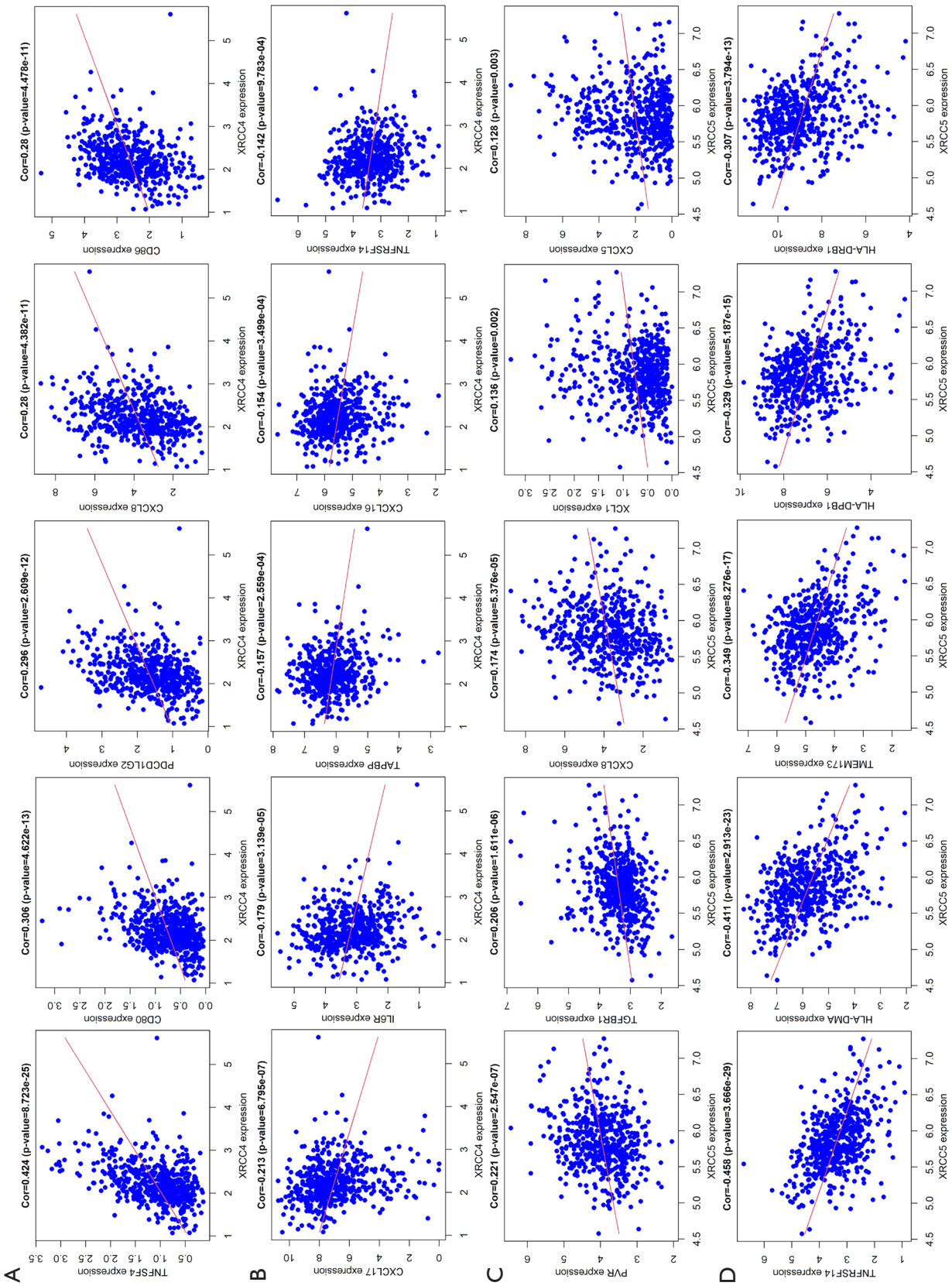

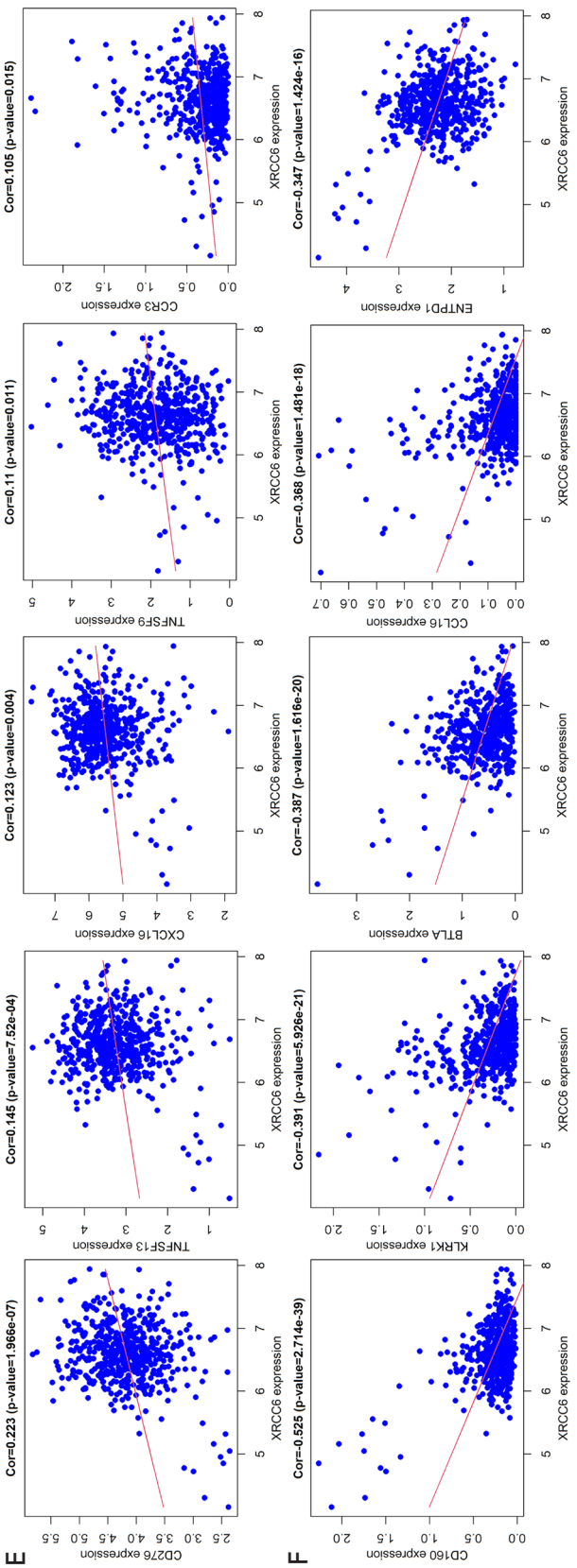

Figure 7 *XRCC4*, *XRCC5*, and *XRCC6* of *XRCC* genes were correlated to immune markers in LUAD. LUAD, lung adenocarcinoma.

and PRKDC increased in unpaired and paired LUAD tissues. ROC analysis showed that the AUCs of XRCC1, XRCC6, XRCC2, XRCC3, FANCG, XRCC4, XRCC5, and PRKDC were all between 0.5 and 1. Cox regression analysis demonstrated that XRCC4, XRCC5 and XRCC6 were independent risk factors affecting the prognosis of LUAD patients. Kaplan-Meier survival analysis showed that the prognosis of LUAD patients in the high-risk group was worse, and a high-risk score was significantly correlated with the gender, clinical stage, T stage, N stage, M stage, and survival status of LUAD patients. These results indicated that XRCC4, XRCC5, and XRCC6 play an important role in the progression of LUAD and are expected to become biomarkers for the diagnosis and prognosis of LUAD. Muylaert *et al.* reported that DNA ligase IV/XRCC4 plays a crucial role in the herpesvirus replication cycle. Reducing DNA ligase IV/XRCC4 could inhibit herpes simplex virus type I DNA replication (28). The expression of Ku86 (XRCC5) is significantly increased in serous ovarian cancer (SOC), and down-regulation of Ku86 expression could promote increased γ-H2AX expression, resulting in the inhibition of cell proliferation, cell cycle block in G2 phase, and the increase of G2/G1. X-ray irradiation could also reduce the expression of Ku86 to promote the above biological effects, and increase the expression of γ-H2AX (29). XRCC6 is overexpressed in human osteosarcoma tissues and cells. The high expression of XRCC6 is related to the clinical stage and tumor size of patients with osteosarcoma. The decreased expression of XRCC6 could inhibit the proliferation of osteosarcoma cells through G2/M phase arrest, which might regulate the growth of osteosarcoma through β-catenin/Wnt signaling pathway (30). The *XRCC* genes were related factors of DNA damage repair, and the risk model based on XRCC4, XRCC5, and XRCC6 could involve mitotic metaphase plate congression, DNA replication, RNA degradation, the cell cycle, oocyte meiosis, basal transcription factors, DNA replication, and so on. This indicates that XRCC4, XRCC5, and XRCC6 are related to cell cycle, DNA damage and DNA replication; however, further confirmation by basic research is needed.

It is well known that the progression of cancer is related to factors in the immune microenvironment. For example, C-X-C motif chemokine ligand 8 (CXCL8) is associated with a high tumor burden in LUAD and is negatively correlated with DACH1 expression. High DACH1 expression and low CXCL8 expression has been found to prolong the time of death and tumor recurrence

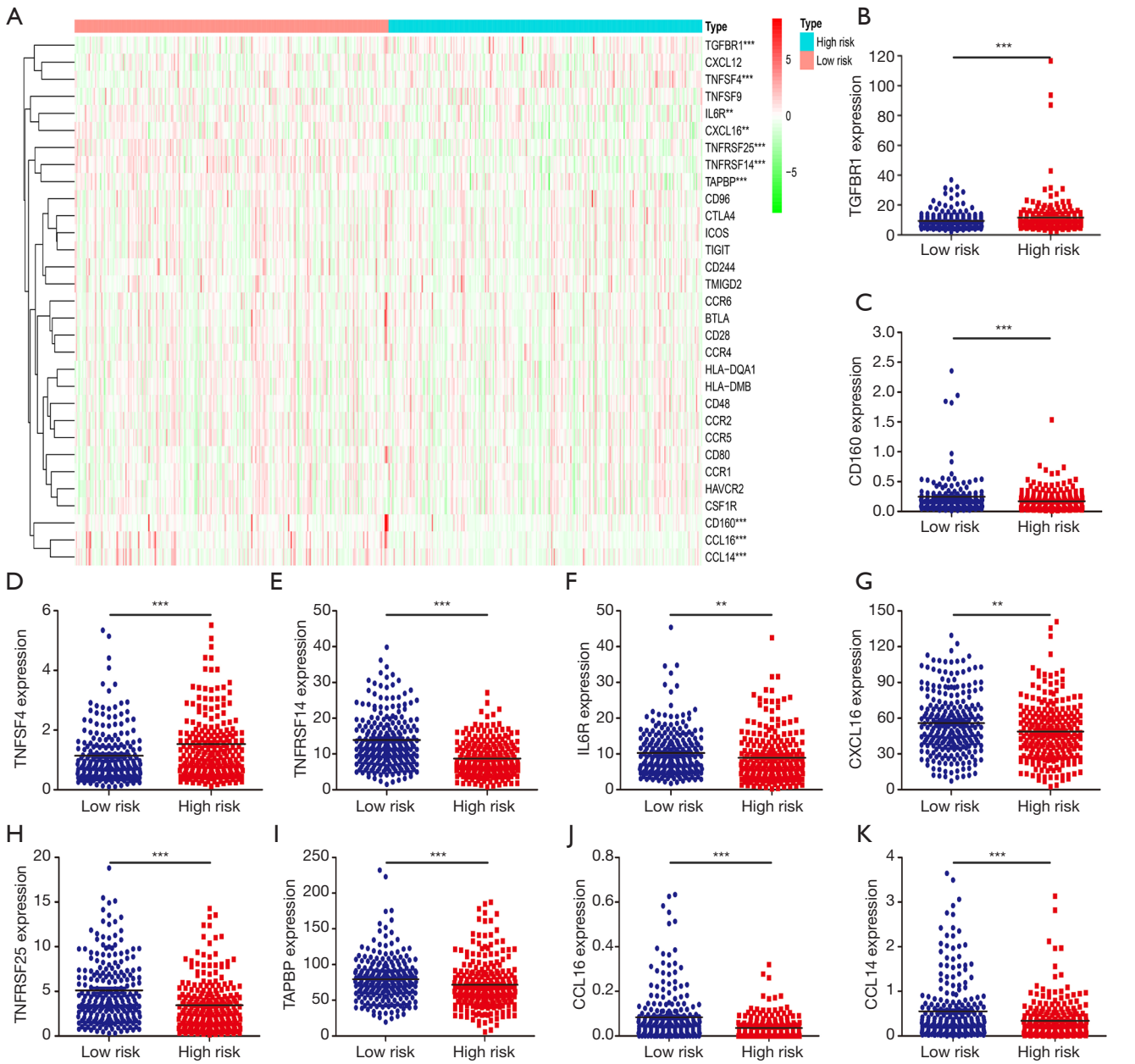

Figure 8 Risk score was correlated to immune markers based on XRCC4, XRCC5, and XRCC6 in LUAD. **, P<0.01; ***, P<0.001. LUAD, lung adenocarcinoma.

of patients. DACH1 can inhibit the activity of the CXCL8 promoter and reduce the level of CXCL8 expression through transcription at the sites of activating protein-1 (AP-1) and nuclear factor-κB (NF-κB) (31). We found that the expression level of XRCC4 was correlated with the expression levels of TNFSF4, CD80, PDCD1LG2, CXCL8, CXCL17, IL6R, TAPBP, CXCL16, and so on; the expression level of XRCC5 was correlated with the expression levels of PVR, TGFBR1, CXCL8, XCL1, TNFRSF14, HLA-DMA, TMEM173, HLA-DPB1, and so on; and the expression level of XRCC6 was correlated with the expression level of CD276, TNFSF13, CXCL16, TNFSF9, CD160, KLRK1, BTLA, CCL16, and so on. In the high- and low-risk groups, it was found that

the expression levels of TGFBR1, CD160, TNFSF4, TNFRSF14, IL6R, CXCL16, TNFRSF25, TAPBP, CCL16, and CCL14 were significantly correlated with a high risk. Meanwhile, Jiang *et al.* reported that TGFBR1, TNFSF4, and IL6R were associated with lung cancer progression (32-35), which provided some evidence for our research.

The risk model based on TCGA data has good prognostic value. However, clinical tissue samples should be collected to verify the expression of XRCC4/5/6 in LUAD tissues via the RT-PCR and western-blot, and the value of XRCC4/5/6 in the diagnosis and prognosis of LUAD was analyzed. In addition, we need to build cell models in the future to explore the cell growth, migration and singaling mechanisms of XRCC4/5/6 in the progression of LUAD. Generally speaking, the *XRCC* genes played an important role in the diagnosis and prognosis of LUAD. XRCC4, XRCC5, and XRCC6 were independent risk factors affecting the prognosis of LUAD patients. There were significant differences in prognosis, sex, clinical stage, T stage, N stage, M stage, and survival status of LUAD patients in the high- and low-risk groups. The clinical stage and risk score were independent risk factors for poor prognosis in patients with LUAD. The risk model was involved in mitotic metaphase plate congression, RNA degradation, cell cycle, oocyte meiosis, basal transcription factors, DNA replication, and other processes. XRCC4, XRCC5, XRCC6, and the risk scores were significantly correlated with the expression levels of immune factors of TGFBR1, CD160, TNFSF4, TNFRSF14, IL6R, CXCL16, TNFRSF25, TAPBP, CCL16, and CCL14.

Conclusions

In this study, the risk model based on XRCC4, XRCC5, and XRCC6 could predict the progression of LUAD patients.

Acknowledgments

Funding: Science and Technology Development Foundation of Xiaoping Chen (CXPJJH12000002-20200), Annual Fund Project of Hubei University of Medical (2019JJXM073), and Office issued of Shiyan Taihe Hospital [2021] No. 83(2021LC+JC103).

Footnote

Reporting Checklist: The authors have completed the TRIPOD reporting checklist. Available at https://dx.doi.org/10.21037/tcr-21-1431

Conflicts of Interest: All authors have completed the ICMJE uniform disclosure form (available at https://dx.doi.org/10.21037/tcr-21-1431). The authors have no conflicts of interest to declare.

Ethical Statement: The authors are accountable for all aspects of the work in ensuring that questions related to the accuracy or integrity of any part of the work are appropriately investigated and resolved. The study was conducted in accordance with the Declaration of Helsinki (as revised in 2013). Institutional ethical approval and informed consent were waived.

References

1. Na R, Wu Y, Jiang G, et al. Germline mutations in DNA repair genes are associated with bladder cancer risk and unfavourable prognosis. BJU Int 2018;122:808-13.
2. De Gregoriis G, Ramos JA, Fernandes PV, et al. DNA repair genes PAXIP1 and TP53BP1 expression is associated with breast cancer prognosis. Cancer Biol Ther 2017;18:439-49.
3. Jhuraney A, Woods NT, Wright G, et al. PAXIP1 Potentiates the Combination of WEE1 Inhibitor AZD1775 and Platinum Agents in Lung Cancer. Mol Cancer Ther 2016;15:1669-81.
4. Crowe DL, Lee MK. New role for nuclear hormone receptors and coactivators in regulation of BRCA1-mediated DNA repair in breast cancer cell lines. Breast Cancer Res 2006;8:R1.
5. Li J, Zhang J, Liu Y, et al. Increased expression of DNA repair gene XPF enhances resistance to hydroxycamptothecin in bladder cancer. Med Sci Monit 2012;18:BR156-62.
6. Rizeq B, Sif S, Nasrallah GK, et al. Novel role of BRCA1

interacting C-terminal helicase 1 (BRIP1) in breast tumour cell invasion. J Cell Mol Med 2020;24:11477-88.
7. Abdel-Fatah T, Sultana R, Abbotts R, et al. Clinicopathological and functional significance of XRCC1 expression in ovarian cancer. Int J Cancer 2013;132:2778-86.
8. Qin CJ, Song XM, Chen ZH, et al. XRCC2 as a predictive biomarker for radioresistance in locally advanced rectal cancer patients undergoing preoperative radiotherapy. Oncotarget 2015;6:32193-204.
9. Ke D, Guo Q, Fan TY, et al. Analysis of the Role and Regulation Mechanism of hsa-miR-147b in Lung Squamous Cell Carcinoma Based on The Cancer Genome Atlas Database. Cancer Biother Radiopharm 2021;36:280-91.
10. Liu H, Qiu C, Wang B, et al. Evaluating DNA Methylation, Gene Expression, Somatic Mutation, and Their Combinations in Inferring Tumor Tissue-of-Origin. Front Cell Dev Biol 2021;9:619330.
11. Chen H, Luo J, Guo J. Development and validation of a five-immune gene prognostic risk model in colon cancer. BMC Cancer 2020;20:395.
12. Lyu Z, Li N, Chen S, et al. Risk prediction model for lung cancer incorporating metabolic markers: Development and internal validation in a Chinese population. Cancer Med 2020;9:3983-94.
13. Rhodes DR, Kalyana-Sundaram S, Mahavisno V, et al. Oncomine 3.0: genes, pathways, and networks in a collection of 18,000 cancer gene expression profiles. Neoplasia 2007;9:166-80.
14. Wang J, Zhang C, He W, et al. Effect of m6A RNA Methylation Regulators on Malignant Progression and Prognosis in Renal Clear Cell Carcinoma. Front Oncol 2020;10:3.
15. Zhu J, Wang M, Hu D. Deciphering N6-Methyladenosine-Related Genes Signature to Predict Survival in Lung Adenocarcinoma. Biomed Res Int 2020;2020:2514230.
16. Zhuang Z, Li Y, Hong Y, et al. A novel prognostic score based on systemic inflammatory biomarkers for patients with oral squamous cell carcinoma. Oral Dis 2021. doi: 10.1111/odi.13774. [Epub ahead of print].
17. Guo Q, Li D, Luo X, et al. The Regulatory Network and Potential Role of LINC00973-miRNA-mRNA ceRNA in the Progression of Non-Small-Cell Lung Cancer. Front Immunol 2021;12:684807.
18. Ma X, Tao R, Li L, et al. Identification of a 5-microRNA signature and hub miRNA-mRNA interactions associated with pancreatic cancer. Oncol Rep 2019;41:292-300.
19. Li D, Ji YM, Guo JL, et al. Upregulated expression of MTFR2 as a novel biomarker predicts poor prognosis in hepatocellular carcinoma by bioinformatics analysis. Future Oncol 2021;17:3187-201.
20. Guo Q, Ke XX, Fang SX, et al. PAQR3 Inhibits Non-small Cell Lung Cancer Growth by Regulating the NF-κB/p53/Bax Axis. Front Cell Dev Biol 2020;8:581919.
21. Santana T, Sá MC, de Moura Santos E, et al. DNA base excision repair proteins APE-1 and XRCC-1 are overexpressed in oral tongue squamous cell carcinoma. J Oral Pathol Med 2017;46:496-503.
22. Liu ZH, Wang N, Wang FQ, et al. High expression of XRCC5 is associated with metastasis through Wnt signaling pathway and predicts poor prognosis in patients with hepatocellular carcinoma. Eur Rev Med Pharmacol Sci 2019;23:7835-47.
23. Niu Y, Zhang X, Zheng Y, et al. XRCC1 deficiency increased the DNA damage induced by γ-ray in HepG2 cell: Involvement of DSB repair and cell cycle arrest. Environ Toxicol Pharmacol 2013;36:311-9.
24. Gao Y, Ferguson DO, Xie W, et al. Interplay of p53 and DNA-repair protein XRCC4 in tumorigenesis, genomic stability and development. Nature 2000;404:897-900.
25. Singh A, Singh N, Behera D, et al. Polymorphism in XRCC1 gene modulates survival and clinical outcomes of advanced North Indian lung cancer patients treated with platinum-based doublet chemotherapy. Med Oncol 2017;34:64.
26. Shao N, Jiang WY, Qiao D, et al. An updated meta-analysis of XRCC4 polymorphisms and cancer risk based on 31 case-control studies. Cancer Biomark 2012-2013;12:37-47.
27. Osawa K, Nakarai C, Uchino K, et al. XRCC3 gene polymorphism is associated with survival in Japanese lung cancer patients. Int J Mol Sci 2012;13:16658-67.
28. Muylaert I, Elias P. Knockdown of DNA ligase IV/XRCC4 by RNA interference inhibits herpes simplex virus type I DNA replication. J Biol Chem 2007;282:10865-72.
29. Ma Q, Kai J, Liu Y, et al. Targeting Ku86 enhances X-ray-induced radiotherapy sensitivity in serous ovarian cancer cells. Int J Biochem Cell Biol 2020;121:105705.
30. Zhu B, Cheng D, Li S, et al. High Expression of XRCC6 Promotes Human Osteosarcoma Cell Proliferation through the β-Catenin/Wnt Signaling Pathway and Is Associated with Poor Prognosis. Int J Mol Sci 2016;17:1188.
31. Liu Q, Li A, Yu S, et al. DACH1 antagonizes CXCL8

to repress tumorigenesis of lung adenocarcinoma and improve prognosis. J Hematol Oncol 2018;11:53.
32. Jiang F, Yu Q, Chu Y, et al. MicroRNA-98-5p inhibits proliferation and metastasis in non-small cell lung cancer by targeting TGFBR1. Int J Oncol 2019;54:128-38.
33. Li Y, Chen Y, Miao L, et al. Stress-induced upregulation of TNFSF4 in cancer-associated fibroblast facilitates chemoresistance of lung adenocarcinoma through inhibiting apoptosis of tumor cells. Cancer Lett 2021;497:212-20.
34. Lei Y, Zang R, Lu Z, et al. ERO1L promotes IL6/sIL6R signaling and regulates MUC16 expression to promote CA125 secretion and the metastasis of lung cancer cells. Cell Death Dis 2020;11:853.
35. Liang K, Liu Y, Eer D, et al. High CXC Chemokine Ligand 16 (CXCL16) Expression Promotes Proliferation and Metastasis of Lung Cancer via Regulating the NF-κB Pathway. Med Sci Monit 2018;24:405-11.

(English Language Editor: A. Kassem)

Cite this article as: Zhang QX, Yang Y, Yang H, Guo Q, Guo JL, Liu HS, Zhang J, Li D. The roles of risk model based on the 3-XRCC genes in lung adenocarcinoma progression. Transl Cancer Res 2021;10(10):4413-4431. doi: 10.21037/tcr-21-1431

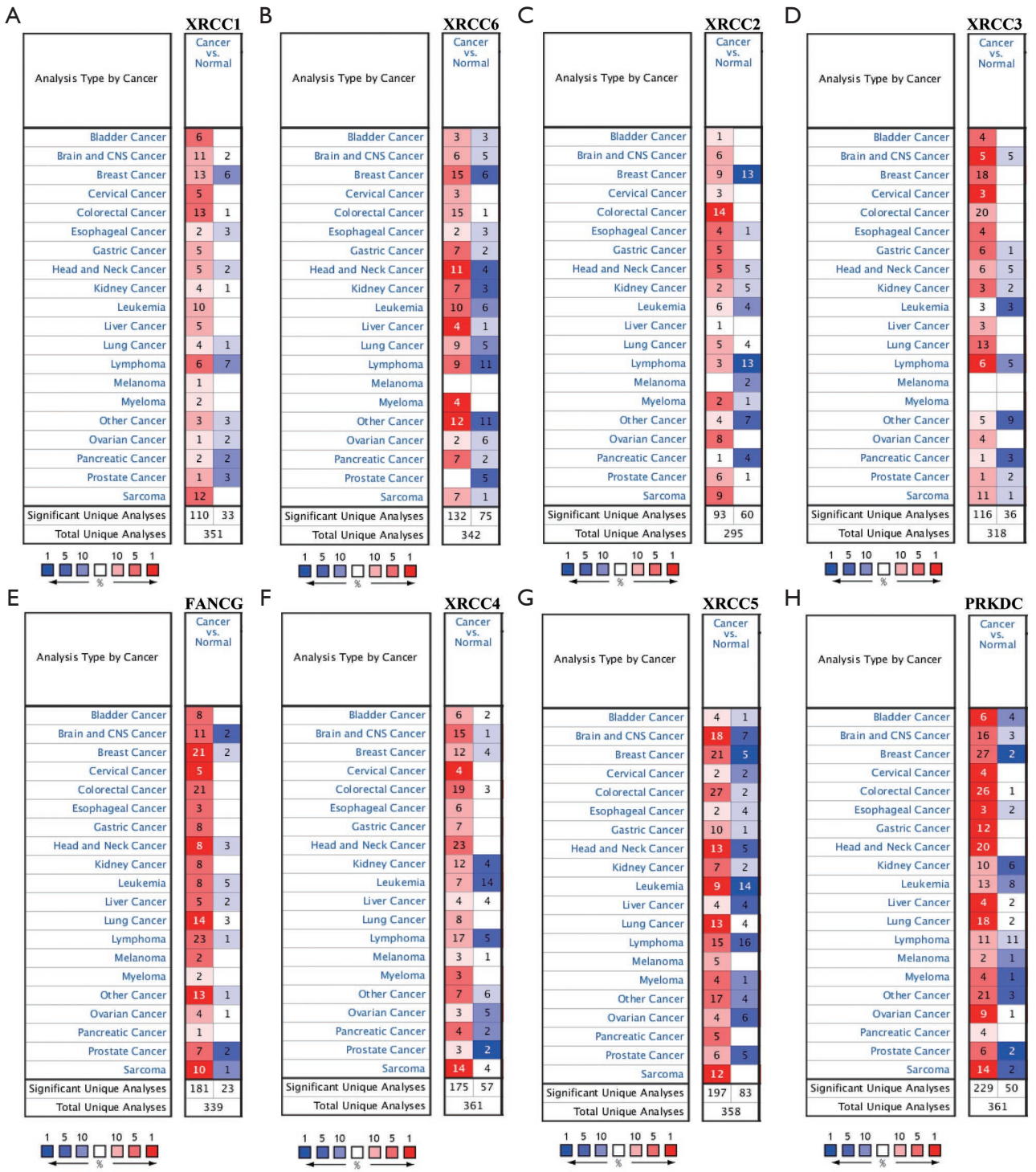

Figure S1 Expression level of XRCC family members in pan-cancer tissues in the Oncomine database. (A) XRCC1; (B) XRCC6; (C) XRCC2; (D) XRCC3; (E) FANCG; (F) XRCC4; (G) XRCC5; (H) PRKDC.

https://dx.doi.org/10.21037/tcr-21-1431

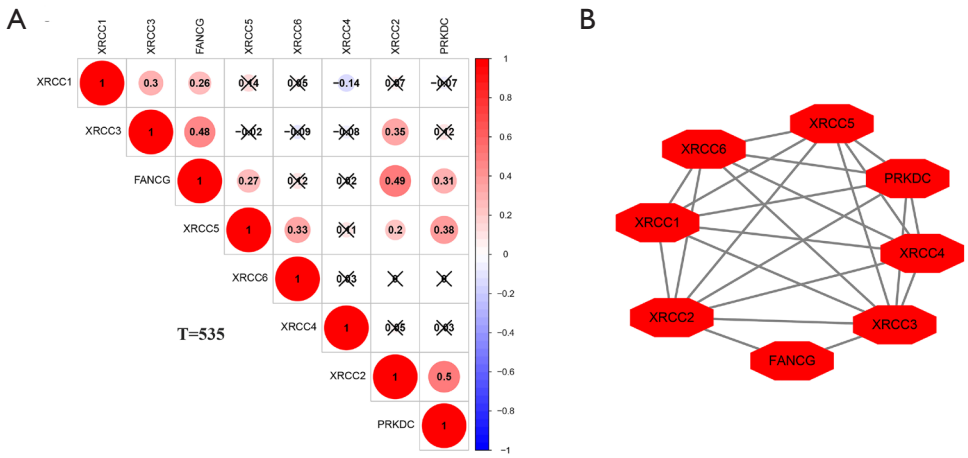

Figure S2 Correlation and functional relationship of the eight members of the *XRCC* family. (A) Correlation analysis; (B) PPI network. PPI, protein-protein interaction.

https://dx.doi.org/10.21037/tcr-21-1431

Table S1 Genes of the *XRCC* family were involved in molecular biological functions

Type	GO	Description	P
BP	GO:0006302	Double-strand break repair	2.94E-11
BP	GO:0006281	DNA repair	3.49E-11
BP	GO:0006310	DNA recombination	3.49E-11
BP	GO:0010212	Response to ionizing radiation	7.62E-10
BP	GO:0009314	Response to radiation	1.68E-09
BP	GO:0006303	Double-strand break repair via nonhomologous end joining	2.33E-09
BP	GO:0009628	Response to abiotic stimulus	4.44E-09
BP	GO:0000723	Telomere maintenance	1.31E-08
BP	GO:0010165	Response to X-ray	3.56E-08
BP	GO:0010332	Response to gamma radiation	2.12E-07
BP	GO:0075713	Establishment of integrated proviral latency	2.84E-07
BP	GO:0006266	DNA ligation	1.33E-06
BP	GO:0006312	Mitotic recombination	2.32E-06
BP	GO:0071475	Cellular hyperosmotic salinity response	3.91E-05
BP	GO:0032481	Positive regulation of type I interferon production	5.69E-05
BP	GO:0000707	Meiotic DNA recombinase assembly	0.00012
BP	GO:0000724	Double-strand break repair via homologous recombination	0.00012
BP	GO:0051351	Positive regulation of ligase activity	0.00012
BP	GO:0042148	Strand invasion	0.00013
BP	GO:0000722	Telomere maintenance via recombination	0.00019
BP	GO:0051103	DNA ligation involved in DNA repair	0.00019
BP	GO:0071481	Cellular response to X-ray	0.00019
BP	GO:0048660	Regulation of smooth muscle cell proliferation	0.00021
BP	GO:0006996	Organelle organization	0.00024
BP	GO:0002218	Activation of innate immune response	0.00057
BP	GO:0071480	Cellular response to gamma radiation	0.00069
BP	GO:0007420	Brain development	0.00087
BP	GO:0032205	Negative regulation of telomere maintenance	0.0012
BP	GO:0007131	Reciprocal meiotic recombination	0.0017
BP	GO:0036297	Interstrand cross-link repair	0.0017
BP	GO:0032508	DNA duplex unwinding	0.002
BP	GO:0033044	Regulation of chromosome organization	0.002
BP	GO:0001756	Somitogenesis	0.0027
BP	GO:0043902	Positive regulation of multi-organism process	0.0035
BP	GO:0002244	Hematopoietic progenitor cell differentiation	0.0037
BP	GO:0007399	Nervous system development	0.0054
BP	GO:0080134	Regulation of response to stress	0.0074
BP	GO:0022414	Reproductive process	0.0083
BP	GO:0043085	Positive regulation of catalytic activity	0.0086
BP	GO:0051704	Multi-organism process	0.0086
BP	GO:0048731	System development	0.01
BP	GO:0045087	Innate immune response	0.0114
BP	GO:0051240	Positive regulation of multicellular organismal process	0.0118
BP	GO:0048513	Animal organ development	0.015
BP	GO:0051054	Positive regulation of DNA metabolic process	0.0163
BP	GO:0031399	Regulation of protein modification process	0.0169
BP	GO:0045935	Positive regulation of nucleobase-containing compound metabolic process	0.0176
BP	GO:0048522	Positive regulation of cellular process	0.0207
BP	GO:0022402	Cell cycle process	0.0213
BP	GO:0045321	Leukocyte activation	0.0213
BP	GO:0048584	Positive regulation of response to stimulus	0.0268
BP	GO:1901990	Regulation of mitotic cell cycle phase transition	0.0354
BP	GO:0051172	Negative regulation of nitrogen compound metabolic process	0.0381
BP	GO:0031324	Negative regulation of cellular metabolic process	0.0454
BP	GO:0050769	Positive regulation of neurogenesis	0.0469
BP	GO:0051094	Positive regulation of developmental process	0.0475
MF	GO:0140097	Catalytic activity, acting on DNA	2.35E-07
MF	GO:0003684	Damaged DNA binding	3.37E-07
MF	GO:0008094	DNA-dependent ATPase activity	3.37E-07
MF	GO:0003677	DNA binding	6.46E-05
MF	GO:0000150	Recombinase activity	0.0001
MF	GO:0003690	Double-stranded DNA binding	0.0001
MF	GO:0008022	Protein C-terminus binding	0.00044
MF	GO:0005524	ATP binding	0.00074
MF	GO:0042162	Telomeric DNA binding	0.00074
MF	GO:0003678	DNA helicase activity	0.00078
MF	GO:0008144	Drug binding	0.00088
MF	GO:0003697	Single-stranded DNA binding	0.0019
MF	GO:0016787	Hydrolase activity	0.003
MF	GO:0003824	Catalytic activity	0.0188
MF	GO:0005488	Binding	0.0385
CC	GO:1990391	DNA repair complex	6.40E-11
CC	GO:0070419	Nonhomologous end joining complex	2.57E-10
CC	GO:0000784	Nuclear chromosome, telomeric region	8.13E-08
CC	GO:0005654	Nucleoplasm	1.10E-05
CC	GO:0043564	Ku70:Ku80 complex	1.10E-05
CC	GO:0005958	DNA-dependent protein kinase-DNA ligase 4 complex	1.97E-05
CC	GO:0033063	Rad51B-Rad51C-Rad51D-XRCC2 complex	2.58E-05
CC	GO:0005730	Nucleolus	6.28E-05
CC	GO:0005694	Chromosome	6.31E-05
CC	GO:0032991	Protein-containing complex	6.31E-05
CC	GO:0000783	Nuclear telomere cap complex	6.43E-05
CC	GO:0032993	Protein-DNA complex	0.00015
CC	GO:0043232	Intracellular non-membrane-bounded organelle	0.00028
CC	GO:0005657	Replication fork	0.00056
CC	GO:0005829	Cytosol	0.0111
CC	GO:0005667	Transcription regulator complex	0.0162
CC	GO:0034774	Secretory granule lumen	0.0162

https://dx.doi.org/10.21037/tcr-21-1431

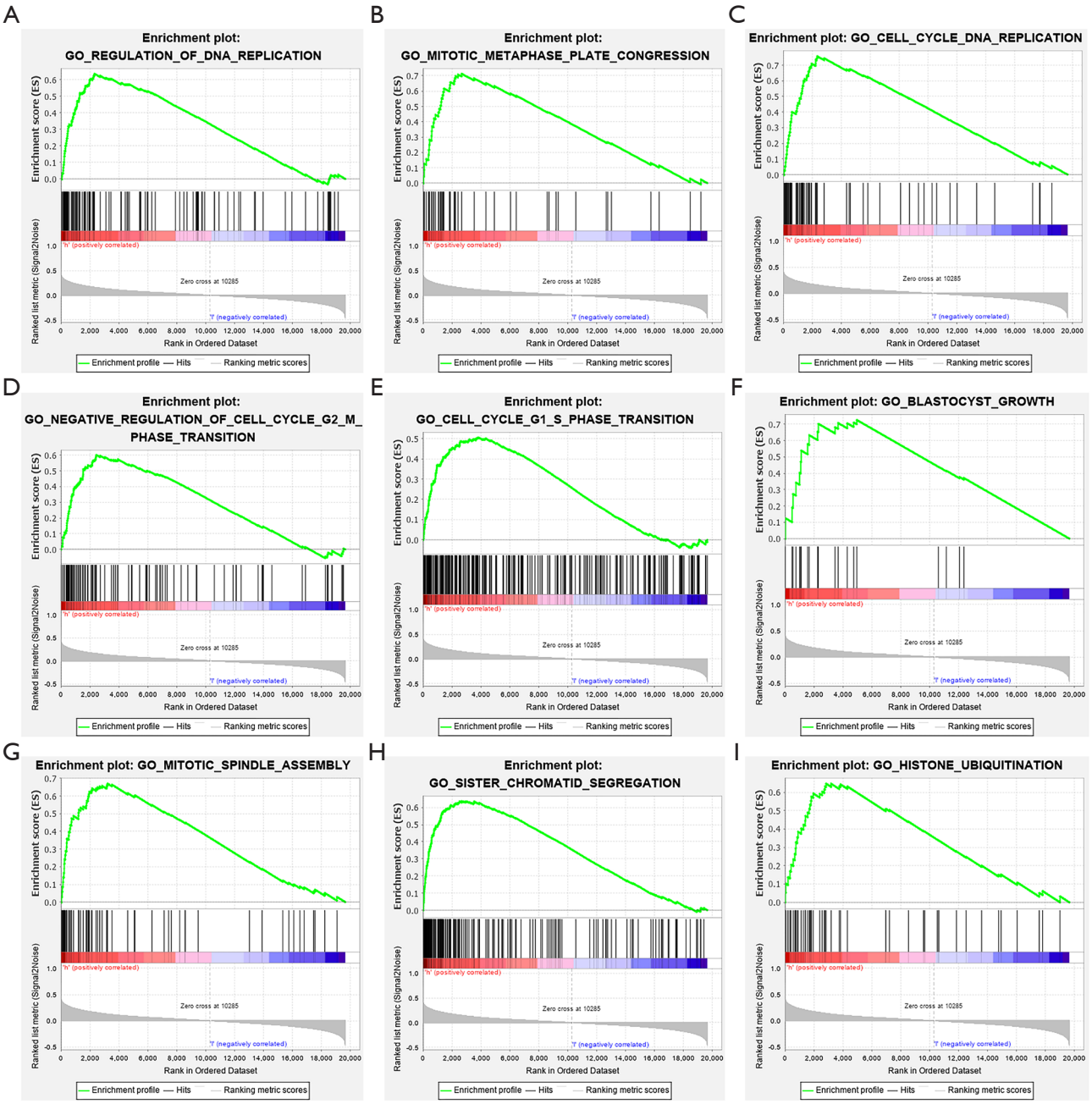

Figure S3 The biological functions involved in the high-risk model.

https://dx.doi.org/10.21037/tcr-21-1431

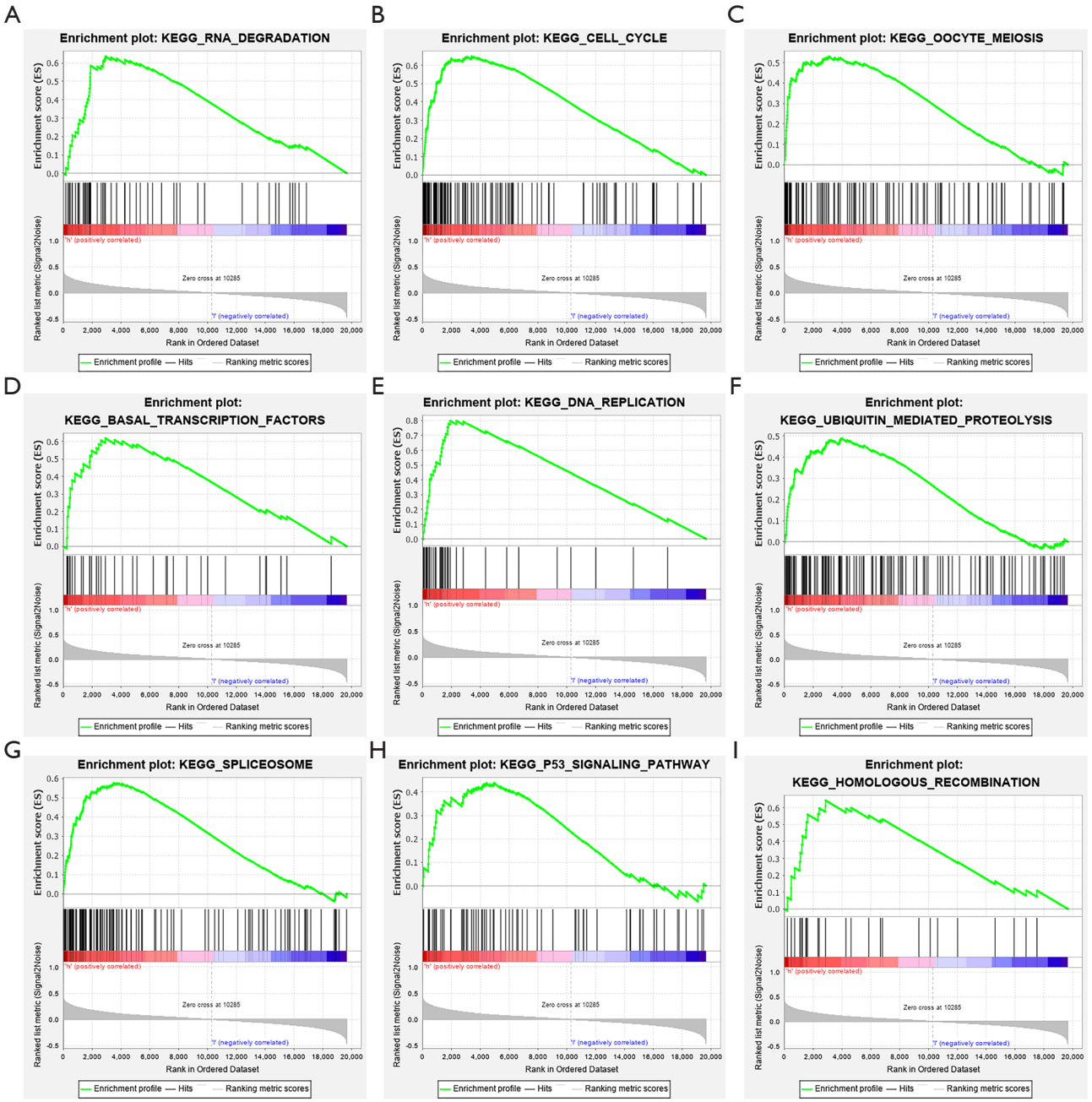

Figure S4 The signaling pathways involved in the high-risk model.

https://dx.doi.org/10.21037/tcr-21-1431

Table S2 *XRCC4*, *XRCC5*, and *XRCC6* were related to the immune genes

XRCC4	cor	P	XRCC5	cor	P	XRCC6	cor	P
CX3CL1	0.025	0.568931297	CX3CL1	-0.292	5.98E-12	CX3CL1	-0.023	0.591492333
CCL26	0.233	4.99E-08	CCL26	0.057	0.186796344	CCL26	-0.024	0.585938933
TNFRSF17	0.169	8.17E-05	TNFRSF17	-0.06	0.165506718	TNFRSF17	-0.157	0.000265563
TNFRSF9	0.248	5.77E-09	TNFRSF9	-0.045	0.302695211	TNFRSF9	-0.128	0.003092972
PVR	0.004	0.920944752	PVR	0.221	2.55E-07	PVR	0.082	0.059349591
XRCC5	0.175	4.87E-05	XRCC5	1	0	XRCC5	0.357	1.46E-17
CXCL2	-0.035	0.419462461	CXCL2	-0.264	5.44E-10	CXCL2	-0.214	5.75E-07
LAG3	-0.008	0.852057213	LAG3	-0.065	0.133636238	LAG3	-0.149	0.000538555
CD40	0.129	0.002888207	CD40	-0.176	4.39E-05	CD40	-0.065	0.130786826
TNFSF13B	0.262	7.13E-10	TNFSF13B	-0.012	0.784919029	TNFSF13B	-0.149	0.000527802
CCL22	0.062	0.152716365	CCL22	-0.163	0.000151071	CCL22	-0.002	0.96585854
CCL17	0.034	0.434880902	CCL17	-0.257	1.53E-09	CCL17	0.021	0.620604918
CD276	-0.007	0.867022858	CD276	0.109	0.011950511	CD276	0.223	1.97E-07
CCL24	0.212	7.08E-07	CCL24	0.118	0.00614055	CCL24	0.03	0.49395181
TGFBR1	0.276	8.77E-11	TGFBR1	0.206	1.61E-06	TGFBR1	-0.188	1.19E-05
CXCL12	0.121	0.004992095	CXCL12	-0.116	0.007292657	CXCL12	-0.143	0.000877105
CCL7	0.249	5.53E-09	CCL7	0.085	0.05048319	CCL7	0.057	0.185472508
CCL2	0.235	3.66E-08	CCL2	-0.08	0.063822772	CCL2	-0.049	0.254718295
CCL8	0.253	3.06E-09	CCL8	0.07	0.107334423	CCL8	0.023	0.60019873
CCL1	0.105	0.014715748	CCL1	-0.061	0.158268068	CCL1	0.027	0.535593895
ULBP1	-0.035	0.421271558	ULBP1	0.013	0.761033993	ULBP1	0.035	0.423845066
CCR6	0.099	0.021528102	CCR6	-0.124	0.003963097	CCR6	-0.274	1.24E-10
CD86	0.28	4.48E-11	CD86	-0.071	0.101435478	CD86	-0.156	0.000293129
HHLA2	0.055	0.20585345	HHLA2	-0.138	0.001384266	HHLA2	0.011	0.795640807
CCL20	0.118	0.006493886	CCL20	0.036	0.408983419	CCL20	-0.039	0.364853416
CD48	0.163	0.00015073	CD48	-0.101	0.019605336	CD48	-0.142	0.000978132
CD160	0.116	0.007319177	CD160	-0.144	0.000848341	CD160	-0.525	2.71E-39
TNFSF4	0.424	8.72E-25	TNFSF4	0.098	0.022970244	TNFSF4	-0.155	0.000312759
CD274	0.247	7.21E-09	CD274	-0.078	0.070230227	CD274	-0.175	4.80E-05
TNFSF18	0.216	4.42E-07	TNFSF18	0.04	0.361341843	TNFSF18	-0.074	0.08598465
TNFRSF8	0.065	0.132654552	TNFRSF8	-0.062	0.149570582	TNFRSF8	-0.1	0.020539666
CD80	0.306	4.62E-13	CD80	-0.096	0.027015198	CD80	-0.302	1.01E-12
CCR2	0.186	1.47E-05	CCR2	-0.115	0.007703775	CCR2	-0.21	9.64E-07
CXCR4	0.14	0.001129742	CXCR4	-0.086	0.047195645	CXCR4	-0.201	2.74E-06
CD244	0.123	0.004337248	CD244	-0.104	0.016244471	CD244	-0.205	1.68E-06
CXCL6	0.09	0.036807951	CXCL6	0.051	0.243105359	CXCL6	-0.077	0.075924369
KIR2DL1	0.015	0.725185178	KIR2DL1	0.062	0.152641661	KIR2DL1	-0.017	0.70244992
TNFSF9	0.176	4.23E-05	TNFSF9	-0.139	0.001241306	TNFSF9	0.11	0.010826689
CD70	0.127	0.00335312	CD70	-0.015	0.728667018	CD70	0.033	0.444863555
TNFSF14	0.018	0.679743896	TNFSF14	-0.208	1.25E-06	TNFSF14	-0.271	1.86E-10
CCR7	-0.022	0.604451231	CCR7	-0.214	5.73E-07	CCR7	-0.199	3.40E-06
KDR	0.05	0.243942206	KDR	-0.043	0.318860255	KDR	-0.104	0.016601791
ADORA2A	-0.039	0.367768047	ADORA2A	-0.197	4.48E-06	ADORA2A	-0.298	2.10E-12
CCL25	0.079	0.066310209	CCL25	-0.032	0.466143467	CCL25	-0.086	0.046960161
IDO1	0.109	0.01149635	IDO1	0.033	0.450656196	IDO1	-0.054	0.211079429
VTCN1	-0.041	0.34718313	VTCN1	0.033	0.449533403	VTCN1	-0.017	0.69228404
IL2RA	0.237	2.80E-08	IL2RA	0.041	0.338378754	IL2RA	-0.099	0.022629607
KLRC1	0.247	7.43E-09	KLRC1	-0.019	0.656390121	KLRC1	-0.175	4.70E-05
HAVCR2	0.255	2.13E-09	HAVCR2	-0.124	0.004177175	HAVCR2	-0.147	0.000665012
NT5E	0.182	2.34E-05	NT5E	-0.03	0.488995346	NT5E	0.021	0.631090231
IL6	0.17	7.49E-05	IL6	0.02	0.645310115	IL6	-0.107	0.013552203
IL10	0.17	7.50E-05	IL10	-0.055	0.200896624	IL10	-0.101	0.019997271
CCL21	0.093	0.032215511	CCL21	-0.05	0.248700196	CCL21	0.039	0.369975764
ENTPD1	0.239	2.07E-08	ENTPD1	-0.051	0.239693681	ENTPD1	-0.347	1.42E-16
CXCL9	0.084	0.052169796	CXCL9	0.055	0.200980705	CXCL9	-0.115	0.007711904
CD27	0.046	0.28735872	CD27	-0.147	0.000675162	CD27	-0.138	0.001329469
XCL1	0.015	0.734176917	XCL1	0.136	0.001644228	XCL1	0.035	0.419901604
XCL2	0.12	0.005350195	XCL2	-0.051	0.23618319	XCL2	-0.095	0.02843227
CXCL14	0.064	0.13993607	CXCL14	-0.093	0.030958584	CXCL14	-0.067	0.119622165
CCL28	0.147	0.000664186	CCL28	-0.07	0.106788675	CCL28	-0.138	0.001430795
XRCC4	1	0	XRCC4	0.175	4.87E-05	XRCC4	0.003	0.946384078
CD96	0.098	0.023091268	CD96	-0.093	0.030606415	CD96	-0.254	2.54E-09
CXCL13	0.092	0.034174697	CXCL13	-0.021	0.62473293	CXCL13	-0.125	0.00388277
TNFRSF14	-0.142	0.000978329	TNFRSF14	-0.458	3.67E-29	TNFRSF14	-0.22	2.80E-07
TNFRSF13C	-0.051	0.235189406	TNFRSF13C	-0.106	0.013990073	TNFRSF13C	-0.206	1.54E-06
ICOSLG	-0.03	0.488753722	ICOSLG	-0.044	0.307766389	ICOSLG	-0.047	0.275085532
CXCR5	-0.034	0.43758992	CXCR5	-0.123	0.004469894	CXCR5	-0.132	0.002247667
IL6R	-0.179	3.14E-05	IL6R	-0.219	3.23E-07	IL6R	-0.093	0.03123836
CCR5	0.138	0.001415216	CCR5	-0.116	0.007136542	CCR5	-0.256	1.82E-09
CXCL16	-0.154	0.000349931	CXCL16	-0.218	3.55E-07	CXCL16	0.123	0.004295705
TNFSF13	-0.052	0.230723652	TNFSF13	-0.249	5.34E-09	TNFSF13	0.145	0.000751992
CXCR1	0.006	0.890843794	CXCR1	0.045	0.296525679	CXCR1	-0.05	0.252319994
CTLA4	0.159	0.000217081	CTLA4	-0.117	0.006760274	CTLA4	-0.292	5.50E-12
ICOS	0.218	3.59E-07	ICOS	-0.115	0.007588628	ICOS	-0.281	3.48E-11
CXCL3	0.03	0.487640536	CXCL3	-0.124	0.003947719	CXCL3	-0.164	0.000141255
CXCL5	0.21	9.58E-07	CXCL5	0.128	0.002911276	CXCL5	-0.049	0.254691705
CXCL1	0.044	0.309590843	CXCL1	-0.049	0.255340454	CXCL1	-0.136	0.001622125
CCR1	0.213	6.93E-07	CCR1	-0.091	0.034770103	CCR1	-0.135	0.001698474
RAET1E	0.091	0.035354522	RAET1E	0.12	0.005530295	RAET1E	0.022	0.615347732
B2M	0.274	1.07E-10	B2M	-0.04	0.359475197	B2M	-0.001	0.975203616
TMIGD2	0.102	0.018356154	TMIGD2	-0.098	0.02303364	TMIGD2	-0.102	0.018320314
CX3CR1	-0.021	0.625401388	CX3CR1	-0.221	2.35E-07	CX3CR1	-0.076	0.079903969
TAP1	0.158	0.000243567	TAP1	0.094	0.030043655	TAP1	0.039	0.368768465
LGALS9	-0.026	0.549176875	LGALS9	-0.235	3.97E-08	LGALS9	-0.038	0.386501579
CXCL10	0.241	1.55E-08	CXCL10	0.1	0.020707958	CXCL10	-0.038	0.382458495
CXCL11	0.191	8.69E-06	CXCL11	0.056	0.199108316	CXCL11	-0.039	0.364443135
CXCL8	0.28	4.38E-11	CXCL8	0.174	5.38E-05	CXCL8	0.014	0.741802874
CCL11	0.211	8.97E-07	CCL11	0.034	0.433707789	CCL11	-0.038	0.384018567
CXCR6	0.17	7.88E-05	CXCR6	-0.065	0.132557272	CXCR6	-0.261	9.39E-10
CCL19	-0.02	0.641061688	CCL19	-0.154	0.000336546	CCL19	-0.056	0.199618569
XCR1	-0.056	0.197612065	XCR1	-0.149	0.000529835	XCR1	-0.195	5.66E-06
CCR9	0.047	0.276958792	CCR9	-0.095	0.028781645	CCR9	-0.113	0.008798978
CD28	0.208	1.17E-06	CD28	-0.14	0.001163288	CD28	-0.341	4.80E-16
HLA-DQB1	0.008	0.849400934	HLA-DQB1	-0.305	5.44E-13	HLA-DQB1	-0.085	0.04908356
CCR8	0.259	1.21E-09	CCR8	0.007	0.869882953	CCR8	-0.132	0.002207012
CXCR2	0.044	0.312593351	CXCR2	-0.006	0.882801894	CXCR2	-0.115	0.007675023
CCL13	0.247	7.34E-09	CCL13	-0.171	7.09E-05	CCL13	0.059	0.174218653
TNFSF15	-0.129	0.002757172	TNFSF15	-0.074	0.086072179	TNFSF15	-0.035	0.422844781
TIGIT	0.121	0.004900923	TIGIT	-0.09	0.036624257	TIGIT	-0.301	1.25E-12
CSF1R	0.123	0.004502457	CSF1R	-0.158	0.000250205	CSF1R	-0.139	0.001299234
CCR3	0.021	0.620009698	CCR3	-0.04	0.36020986	CCR3	0.105	0.014920839
CCR4	0.102	0.018565906	CCR4	-0.146	0.000697664	CCR4	-0.237	2.84E-08
CCR10	-0.057	0.18778402	CCR10	-0.019	0.66747335	CCR10	-0.009	0.836408466
TMEM173	-0.075	0.08320565	TMEM173	-0.349	8.28E-17	TMEM173	-0.024	0.583184106
BTLA	0.135	0.001819738	BTLA	-0.133	0.002009577	BTLA	-0.387	1.62E-20
CXCR3	-0.024	0.581579106	CXCR3	-0.214	5.98E-07	CXCR3	-0.129	0.002694991
TNFRSF4	-0.012	0.786885943	TNFRSF4	-0.231	6.87E-08	TNFRSF4	-0.043	0.322560803
TNFRSF18	0.001	0.984421798	TNFRSF18	-0.21	9.03E-07	TNFRSF18	-0.027	0.534760723
PDCD1	0.008	0.859882922	PDCD1	-0.119	0.005876848	PDCD1	-0.163	0.000146595
CXCL17	-0.213	6.80E-07	CXCL17	-0.287	1.22E-11	CXCL17	-0.057	0.184694284
HLA-DRB1	0.053	0.224577668	HLA-DRB1	-0.307	3.79E-13	HLA-DRB1	-0.027	0.540222835
XRCC6	0.003	0.946384078	XRCC6	0.357	1.46E-17	XRCC6	1	0
HLA-DQA1	0.09	0.037806709	HLA-DQA1	-0.213	6.43E-07	HLA-DQA1	-0.14	0.001174679
PDCD1LG2	0.296	2.61E-12	PDCD1LG2	0.006	0.884529344	PDCD1LG2	-0.178	3.34E-05
HLA-DOA	0.044	0.305370162	HLA-DOA	-0.224	1.61E-07	HLA-DOA	-0.137	0.001459944
HLA-DMA	-0.026	0.545299624	HLA-DMA	-0.411	2.91E-23	HLA-DMA	-0.075	0.083843037
TAP2	0.115	0.007988396	TAP2	-0.058	0.178166234	TAP2	-0.194	5.87E-06
HLA-DRA	0.155	0.000322511	HLA-DRA	-0.258	1.34E-09	HLA-DRA	-0.059	0.169801594
MICB	0.213	6.66E-07	MICB	0.008	0.855659885	MICB	-0.041	0.345624497
HLA-C	0.038	0.377717168	HLA-C	-0.094	0.029637281	HLA-C	0.093	0.032009771
HLA-E	-0.015	0.727276792	HLA-E	-0.199	3.36E-06	HLA-E	-0.052	0.228742695
HLA-G	0.002	0.968078891	HLA-G	-0.092	0.033520426	HLA-G	-0.011	0.79839848
HLA-F	0.048	0.263498119	HLA-F	-0.213	6.91E-07	HLA-F	-0.075	0.084127372
HLA-A	-0.014	0.745197184	HLA-A	-0.107	0.012955388	HLA-A	0.076	0.078982472
KLRK1	0.052	0.232988983	KLRK1	-0.203	2.30E-06	KLRK1	-0.391	5.93E-21
CCL27	0.004	0.934972608	CCL27	0.016	0.716146069	CCL27	-0.095	0.028784647
TNFRSF25	-0.097	0.024264598	TNFRSF25	-0.212	7.47E-07	TNFRSF25	-0.209	1.12E-06
HLA-DPB1	0.04	0.355897655	HLA-DPB1	-0.329	5.19E-15	HLA-DPB1	-0.084	0.051910985
LTA	0.047	0.274373489	LTA	-0.166	0.000112129	LTA	-0.107	0.01302378
HLA-DPA1	0.097	0.024921717	HLA-DPA1	-0.249	5.42E-09	HLA-DPA1	-0.085	0.050194649
TAPBP	-0.157	0.000255941	TAPBP	-0.185	1.61E-05	TAPBP	-0.114	0.008259627
HLA-B	0.083	0.055576211	HLA-B	-0.142	0.000988665	HLA-B	-0.023	0.598586324
HLA-DQA2	0.12	0.005569242	HLA-DQA2	-0.133	0.002055443	HLA-DQA2	-0.005	0.904231415
TNFRSF13B	-0.074	0.089391736	TNFRSF13B	-0.221	2.50E-07	TNFRSF13B	-0.213	6.64E-07
HLA-DOB	0.067	0.12045494	HLA-DOB	-0.226	1.26E-07	HLA-DOB	-0.126	0.003509809
HLA-DMB	0.153	0.000370276	HLA-DMB	-0.258	1.33E-09	HLA-DMB	-0.106	0.014337445
IL10RB	0.215	5.34E-07	IL10RB	-0.057	0.187888043	IL10RB	0.088	0.042873945
KIR2DL3	0.02	0.641242438	KIR2DL3	0.022	0.613652147	KIR2DL3	-0.04	0.361714531
CCL23	0.097	0.024639325	CCL23	-0.193	7.10E-06	CCL23	0.025	0.569402031
CCL16	-0.099	0.022340704	CCL16	-0.271	1.83E-10	CCL16	-0.368	1.48E-18
CCL4	0.178	3.50E-05	CCL4	-0.029	0.50905053	CCL4	-0.123	0.004481432
CCL18	0.105	0.015211413	CCL18	-0.084	0.053196024	CCL18	0.036	0.406136761
CCL15	0.037	0.396886452	CCL15	0.064	0.138957225	CCL15	0.014	0.745198864
CCL14	-0.125	0.00366806	CCL14	-0.241	1.57E-08	CCL14	-0.164	0.000138902
CCL3	0.166	0.00011067	CCL3	-0.08	0.064157517	CCL3	-0.016	0.715552226

https://dx.doi.org/10.21037/tcr-21-1431